[Electronic Supporting Information to accompany *Catal. Sci. Technol.* manuscript CY-ART-06-2018-001139]

Elucidating the mechanism of the UiO-66-catalyzed sulfide oxidation: Activity and selectivity enhancements through changes in the node coordination environment and solvent

Rungmai Limvorapitux,[1] Haoyuan Chen,[2] Matthew L. Mendonca,[2] Mengtan Liu,[1] Randall Q. Snurr, [2,] and SonBinh T. Nguyen[1,*]*

[1]Department of Chemistry and the Institute for Catalysis in Energy Processes, [2]Department of Chemical and Biological Engineering, Northwestern University, 2145 Sheridan Road, Evanston, Illinois 60208

Table of Contents

S1. Materials and methods

Unless otherwise stated, all reagents were used as received. Zirconium chloride ($ZrCl_4$) was purchased from Strem Chemicals, Inc. (Newburyport, MA). Hydrogen peroxide (H_2O_2, 30 wt % in water), naphthalene, benzoic acid (BzOH), zirconium oxide (ZrO_2), zirconium propoxide ($Zr(OPr)_4$, 70 wt % in *n*-propanol), 1,4-benzenedicarboxylic acid (BDC), methanesulfonic acid, methyl phenyl sulfide, methyl phenyl sulfoxide, methyl phenyl sulfone, maleic acid, and zirconium ICP standards were purchased from Sigma-Aldrich Co., LLC. (St. Louis, MI). Concentrated sulfuric acid was purchased from VWR Scientific, LLC (Chicago, IL). Deuterated dimethylsulfoxide (DMSO-d_6, 99%) was purchased from Cambridge Isotope Laboratories, Inc. (Tewksbury, MA). Ultrapure deionized (DI) water (18.2 MΩ•cm resistivity) was obtained from a Millipore Milli-Q Biocel A10 instrument (Millipore Inc., Billerica, MA). Solvents were purchased from either Sigma-Aldrich Co., LLC. (St. Louis, MI) or Fisher Scientific, Inc. (Pittsburg, PA) and used as received.

Powder X-ray diffraction (PXRD) patterns were collected on a STOE's STADI-MP powder diffractometer (STOE & Cie. Ltd, Darmstadt, Germany) equipped with an asymmetric curved Germanium monochromator (Cu $K_{\alpha 1}$ radiation, λ = 1.54056 Å), a one-dimensional silicon strip detector (MYTHEN2 1K from Dectris AG, Baden, Switzerland), and a line-focused Cu X-ray tube operated at 40 kV and 40 mA. The as-received powder was sandwiched between two acetate foils (polymer substrate with neither Bragg reflections nor broad peaks above 10 degrees) and measured in transmission geometry in a rotating holder. Prior to the measurement, the instrument was calibrated against a NIST Silicon standard (640d). Measurements were made over the range $5° < 2\theta < 53°$ in 4° steps of detector and an exposure time of 10 s per step.

N_2 adsorption and desorption isotherms were measured on a Micromeritics Tristar II 3020 (Micromeritics Instrument Corporation, Norcross, GA) at 77 K. Before each run, samples were activated at 120 °C for 24 h under high vacuum on both Schlenk line and on ASAP 2020 instrument (Micromeritics Instrument Corporation, Norcross, GA). About 40-100 mg of sample was used in each measurement and the BET area was calculated in the region P/P_o = 0.005-0.1.

Inductively coupled plasma optical-emission spectroscopy (ICP-OES) was conducted on a computer-controlled (QTEGRA software v. 2.2) Thermo iCap 7600 Duo ICP-OES (Thermo Fisher Scientific, Waltham, MA) instrument equipped with a SPRINT valve and a CETAC 520ASX autosampler (Teledyne CETAC, Inc., Omaha, NE).

For synthetic work, ^{1}H NMR spectra of products were recorded on a Bruker Avance III 500 MHz (499.4 MHz for ^{1}H) spectrometer (Bruker Biospin Corp., Billerica, MA, USA). ^{1}H chemical shifts are referenced in ppm downfield from tetramethylsilane (TMS, δ scale) using the residual solvent resonances as internal standards.

For obtaining MOF compositions, ^{1}H NMR spectra were recorded on an Agilent DD2 600 MHz spectrometer (Agilent, Santa Clara, CA) equipped with a triple-resonance (HCN) cold probe w/ Z-gradient and a sensitivity of ^{1}H = 4300 and ^{13}C

= 250. ^{1}H NMR chemical shifts are referenced in ppm downfield from tetramethylsilane (TMS, δ scale). Maleic acid was used as an internal standard.
Centrifugation was carried out in an Eppendorf Centrifuge 5804 R, Model AG 22331 (Eppendorf AG, Hamburg, Germany) equipped with an F34-6-38 rotor. All centrifugations were carried out at 5000-6000 rpm (3214-4628 *g*) for 10-20 minutes.

Scanning electron microscopy (SEM) images were obtained at Northwestern University's EPIC/NUANCE facility on a SU8030 FE-SEM microscope (Hitachi High Technologies America, Inc., Dallas, TX) with an acceleration voltage of 10 kV. Prior to imaging, activated MOF samples were coated with Os (18 nm thickness) using a Filgen Osmium Coater Model OPC-60A (Filgen, Inc., Nagoya, Japan). Size measurements were obtained from sample populations of >100 particles, which were used to construct the standard normal distribution plots (mean ± 3 standard deviation units) and the histograms.

Gas chromatography was carried out on an Agilent Technologies 6890N Network GC system (Agilent Technologies, Inc., Santa Clara, CA) equipped with an FID detector. An HP-5 capillary column (30 m × 320 μm × 0.25 μm film thickness) was used to analyze the substrates. Analysis parameters were as follows: initial temperature = 80 °C, initial time = 2 minutes, ramp = 20 °C/min, final temperature = 200 °C, final time = 1 minute. Elution times (min) = 4.4 (methyl phenyl sulfide), 5.3 (naphthalene), 6.3 (methyl phenyl sulfoxide), and 6.8 (methyl phenyl sulfone). The amount of oxidation product was calculated based on calibration curves against naphthalene as an internal standard. Response factors: methyl phenyl sulfide = 0.723, methyl phenyl sulfoxide = 0.790, and methyl phenyl sulfone = 0.771.

S2. Computational methods

All electronic structure calculations were carried out using the Gaussian 09 package (revision D.01). The starting structure of the UiO-66 node was adapted from a previous computational work[S1] and re-optimized. In the UiO-66 node model, one BzO- linker was replaced by one H_2O and one -OH to saturate the coordination of two Zr atoms and balance the charge, according to the experimental stoichiometry (see Table S1). All remaining BzO- linkers were then replaced with HCOO- to reduce the system size and speed up the calculations. All geometry optimizations and transition state searches were performed using density functional theory (DFT) with the B3LYP functional.[S2,S3] The def2-SVP basis set[S4] was used for H, C, N, O, S and Cl atoms while the LANL2DZ basis sets[S5] with effective core potentials were applied to the Zr atoms. The polarizable continuum model (PCM),[S6] with default atomic cavity radii and specific solvents corresponding to experimental conditions was used to model solvation effects. For example, results in Fig. 2 in the manuscript for the uncatalyzed and catalyzed reactions included solvation effects for methanol using the PCM model. Similarly, the free energy for acetonitrile in Table 3 in the manuscript was calculated in implicit acetonitrile solvent using the PCM model. Results for methyl phenyl sulfoxide and methyl phenyl sulfone in Table 3 in the manuscript are in implicit methanol. Vibrational analysis and thermochemistry calculations were performed for all species at the same level of theory. Single-point energy calculations were also carried out to refine the energies of all species, in which the def2-SVP basis set was replaced by the larger def2-TZVP basis set and the DFT-D3 dispersion correction[S7] with Becke-Johnson damping[S8] (D3BJ) was applied. The reported Gibbs free energy of each species was calculated by adding the single-point electronic energy (at B3LYP-D3BJ/def2-TZVP level) and the thermochemistry terms (at B3LYP/def2-SVP level) together.

S3. Synthesis of materials

BzOH-UiO-66 batch 1. This material was made by R.L. following a previously reported literature procedure with minor modifications.[S9] In a 1 L Erlenmeyer flask, BzOH (13.3 g, 108 mmol) was dissolved in DMF (412 mL) by stirring before being combined with $ZrCl_4$ (0.85 g, 3.6 mmol) and BDC (0.54 g, 3.3 mmol). Additonal sonication (~1-5 min) can help with the dissolution of all reagents into a clear solution, which was then partitioned evenly among 8 dram glass vials (25.5 mL each, 16 vials in total). The vials were capped tightly and placed in a preheated oven at 120 °C for 24 h. After being cooled to room temperature, the mixture from each vial was transferred separately into 50 mL centrifuge tubes (16 tubes in total) and the mother liquor was separated from the solid by centrifugation. After decanting the mother liquor, the collected solid was then soaked in fresh DMF (~20 mL/tube) for ~8 h, and pelletized by centrifugation to complete one cycle of washing. This cycle was repeated three times to remove the unreacted starting materials. Half of the crude solid was kept for the synthesis of **HCOOH-UiO-66** (see below), while the rest was redispersed in acetone (~20 mL/tube) to exchange out the DMF, collected by centrifugation, and air-dried overnight. To ensure that no residual DMF remains, the solid was subjected to Soxhlet extration with acetone for ~12 h. The resulting solid was then dried overnight at 120 °C under vacuum to give a white powder (~400 mg) that is then stored at room temperature in a screw-capped vial. For analytical data, see Table S1 (BET area and chemical formula), Figure S2a (NMR data), and Figure S6 (PXRD data). This material was used for the majority of the catalysis studies except for the recycling data (Section S7, Figures S16-17).

BzOH-UiO-66 batch 2. To test the differences in batch-to batch variation, this material was synthesized by M.L and worked up by R.L. following the same protocol as described above. For analytical data, see Table S1 (BET area and formula), Figure S2b (NMR data), and Figure S6 (PXRD data). From these charaterizations, this batch of material is very similar to batch 1. This batch of material was used in the recycling experiments described in Section S6 and Section S7, Figure S16-17.

HCOOH-UiO-66. This material was made by adapting a literature protocol for HCl-treated UiO-66.[S10] Half of the crude **BzOH-UiO-66**, synthesized from the previous experiment, was partitioned evenly into two 100 mL glass vials. DMF (60 mL) was added to each vial and the resulting mixtures were sonicated for 2 min followed by addition of HCl (5 mL of an 8 M aqueous solution). The vials were then capped tightly and swirled briefly before being placed into a preheated oven at 100 °C for 24 h. After being cooled to room temperature, the content of each vial was transferred separately into 50 mL centrifuge tubes and subjected to centrifugation. After decanting the mother liquor, the collected solid was then soaked in fresh DMF (~20 mL/tube) for ~2 h, and pelletized by centrifugation to complete one cycle of washing. This cycle was repeated three times to remove HCl and BzOH. The remaining solid was then redispersed in acetone (~20 mL/tube), collected by centrifugation, and air-dried overnight. To ensure that no residual DMF remains, the solid was subjected to Soxhlet extration with acetone for ~12 h. The resulting solid was then dried overnight at 120 °C under vacuum to give a white powder (~400 mg) that is then stored at room temperature in a screw-capped vial.

decap-UiO-66 batch 1. adapting a literature protocol for HCl-treated UiO-66.[S10] In an 8 dram vial, dry **BzOH-UiO-66** (150 mg) was combined with *n*-butanol (18 mL) and HCl (1.5 mL of an 8 M aqueous solution). The vial was capped tightly and swirled briefly before being placed into a preheated oven at 100 °C for 24 h. After being cooled to room temperature, the mixture was transferred into a 50 mL centrifuge tube and subjected to centrifugation. After decanting the mother liquor, the collected solid was then soaked in fresh *n*-butanol (~20 mL) for ~ 2 h, and pelletized by centrifugation to complete one cycle of washing. This cycle was repeated three times to remove HCl and BzOH. The remaining solid was then redispersed in acetone (~20 mL), collected by centrifugation, and air-dried overnight. To ensure that no residual *n*-butanol remains, the solid was subjected to Soxhlet extration with acetone for ~12 h. The resulting solid was then dried overnight at 120 °C under vacuum to give a white powder that is then stored at room temperature in a screw-capped vial. For analytical data, see Table S1 (BET area and formula), Figure S3a (NMR data), and Figure S6 (PXRD data). This material was used for the majority of the catalysis studies except for the recycling data (Section S7, Figures S18-19).

decap-UiO-66 batch 2. This material was made by by R.L. from **BzOH-UiO-66** batch 2, following the same protocol as described above. For analytical data, see Table S1 (BET area and formula), Figure S3b (NMR data), and Figure S6 (PXRD data). From these charaterizations, this batch of material is very similar to batch 1. This batch of material was used in the recycling experiments described in Section S6 and Section S7, Figures S18-19.

Isolated Zr_6-oxo-hydroxo cluster. This material was made by Dr. Yonghwi Kim following a previously reported literature procedure with a minor modification in the capping agent.[S11,12] In a 100 mL round-bottom flask equipped with a magnetic stir bar, BzOH (16 g, 130 mmol) was dissolved in *n*-propanol (50 mL) by stirring before being combined with $Zr(OPr)_4$ (2.1 mL of a 70 wt % solution in *n*-propanol, 5 mmol). The flask was then attached to a water-cooled reflux condenser and the reaction mixture was brought to reflux for 2 h, during which time precipitate started to form. After cooling down, the precipitate was collected by centrifugation and dried under vacuum overnight to give a white powder that is stored at room temperature in a screw-capped vial.

Perbenzoic acid (BzOOH). This compound was synthesized according to a previously reported literature protocol.[S13] In a 100 mL round-bottom flask equipped with a magnetic stir bar, methanesulfonic acid (14.4 g, 150 mmol) was combined with BzOH (3.7 g, 30 mmol). The stirred suspension was warmed up to 40 °C and H_2O_2 (420 µL of a 30 wt % of solution in water, 41 mmol) was then added dropwise over 1-2 min. After 5 h, the reaction mixture was cooled down to room temperature and combined with ice (10 g). The resulting mixture was treated with saturated aqueous $(NH_4)_2SO_4$ solution (10 mL) before being extracted with CH_2Cl_2 (3 × 10 mL). The combined organic extracts were then washed with saturated aqueous $(NH_4)_2SO_4$ solution (3 ×10 mL), dried over $MgSO_4$, and concentrated by rotary evaporation at room temperature. The collected crude-product was further purified via flash column chromatography on silica gel (3 mm × 15 mm; CH_2Cl_2). Combining the product-containing fractions and removing solvents yielded perbenzoic acid as white solid (27 % of benzoic acid impurity).

S4. Compositional analyses of the MOF and cluster materials

Procedure for the quantitative analysis of the Zr content in MOF and cluster materials. Into a 15 mL polypropylene centrifuge tube, conc. H_2SO_4 (1.5 mL), H_2O_2 (30 wt % in water, 250 µL), and HF (250 µL) were added to a small sample (~1 mg) of the material to be analyzed. The resulting mixture was sonicated until the solution became clear (~1 h). The resulting solution was then transferred to a 50 mL polypropylene centrifuge tube, and diluted with DI water to a final

volume of 30 mL. This solution was then analyzed for Zr by ICP-OES (λ = 339.198, 343.823, 327.305, and 349.621 nm) against a calibration curve of standards with known [Zr]. Data are listed in Table S1.
Caution: HF is very toxic and dangerous to handle without proper safety training. PPE must include Silvershield gloves and goggles. Acid digestions and subsequent dilutions should be carried out in a well-ventilated hood.

Procedure for the quantitative analyses of BDC, BzOH, and HCOOH content in MOF and cluster materials. In a 15 mL polypropylene centrifuge tube, HF (6 µL) and DMSO-*d*$_6$ (114 µL) were added to a small sample (~2 mg) of the material to be analyzed. The resulting mixture was sonicated until the solution became clear (~1 h). Then an aliquot (12 µL, corresponding to ~0.2 mg of sample) of the resulting solution was transferred to an NMR tube along with an aliquot of 12 mM maleic acid (MA) solution in DMSO-*d*$_6$ (50 µL), and fresh DMSO-*d*$_6$ (538 uL). This combined solution was then analyzed by ^{1}H NMR spectroscopy with a 90° pulse using a 50 s delay between scans, which exceed the T1 relaxation time for BDC (3.7 s), MA (2.8 s), and HCOOH (9.9 s). The amount of each substrate was calculated by comparing the integration against a calibration curve of standards with known concentrations (see Figure S1 for calibration curve, and Figures S2-5 for NMR spectra).

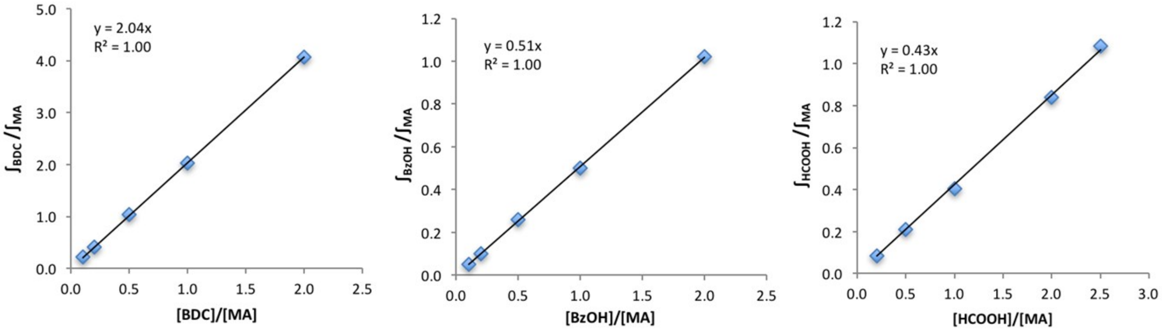

Figure S1. Plots of the concentration ratio of BDC, BzOH, and HCOOH to the MA internal standard versus the integration ratio of the signals for the analytes (BDC, BzOH, and HCOOH) to MA.

The ^{1}H NMR spectra of the digested MOFs can reveal the composition of the organic ligands present in each digested sample. For the **BzOH-UiO-66**, its ^{1}H NMR spectrum confirms the presence of BDC and BzOH (Figure S2), and shows an additional peak for HCOOH, which originates from the decomposition of DMF solvent under the conditions for MOF synthesis. As expected, HCOOH was also found in the **HCOOH-UiO-66** (Figure S4) due to the usage of DMF during the HCl-catalyzed thermal removal of BzOH from **BzOH-UiO-66**. Such HCOOH can readily bind to the open sites of the Zr_6-oxo-hydroxo cluster nodes of UiO-type MOFs, as reported by Lillerud and coworkers.[S14,15] When the BzOH was removed in *n*-butanol instead of DMF, the HCOOH peak was no longer observed in the ^{1}H NMR spectrum of the digested **decap-UiO-66** (Figure S3), further supporting that HCOOH indeed comes from the decomposition of DMF. Finally, the absence of the BzOH peaks in both ^{1}H NMR spectra of **HCOOH-UiO-66** (Figure S4) and **decap-UiO-66** (Figure S3) confirms the successful removal of BzOH in both materials.

Table S1. Formula and BET area of materials.

MOF	Proposed formula[a]	BET area (m^2/g)
Ideal UiO-66	$Zr_6O_4(OH)_4(BDC)_6$	1100[b]
BzOH-UiO-66 batch 1	$Zr_6O_4(OH)_4(BDC)_{3.9}(BzOH)_{2.9}(HCOOH)_{0.3}(\mu_1\text{-}OH)_1(\mu_1\text{-}OH_2)_1$	1490
HCOOH-UiO-66	$Zr_6O_4(OH)_4(BDC)_{3.7}(HCOOH)_{3.9}(\mu_1\text{-}OH)_{0.7}(\mu_1\text{-}OH_2)_{0.7}$	1640
decap-UiO-66 batch 1	$Zr_6O_4(OH)_4(BDC)_{3.7}(\mu_1\text{-}OH)_{4.6}(\mu_1\text{-}OH_2)_{4.6}$	1530[c]
BzOH-UiO-66 batch 2[d]	$Zr_6O_4(OH)_4(BDC)_{4.1}(BzOH)_{3.1}(HCOOH)_{0.1}(\mu_1\text{-}OH)_{0.6}(\mu_1\text{-}OH_2)_{0.6}$	1510
decap -UiO-66 batch 2[d]	$Zr_6O_4(OH)_4(BDC)_{3.6}(\mu_1\text{-}OH)_{4.8}(\mu_1\text{-}OH_2)_{4.8}$	1440[c]
Isolated Zr_6-oxo-hydroxo cluster[e]	$Zr_6O_4(OH)_4(BzOH)_{8.7}(\mu_1\text{-}OH)_{3.3}(\mu_1\text{-}OH_2)_{3.3}$	-

[a]The formula of UiO-66 MOFs are determined from ^{1}H NMR spectra and ICP-OES data of digested materials carried out by R.L. The open sites were proposed to be terminated by μ_1-OH and μ_1-OH_2. [b]This BET area was obtained from a literature report, calculated by fitting simulated N_2 isotherms.[S16] For UiO-66 with 8 linkers per node, the calculated BET area was 1400 m^2/g.[S16] [c]The variation in this data illustrates the differences in materials obtained by the same researcher (R.L.) using the same decapping protocol but from different batches of BzOH-UiO-66 made by two different experimenters (R.L. and M.L.). In fact, a range of 1440-1720 m^2/g has been obtained in our laboratory across three different batches of materials. [d]This batch of material was used in the recyclability experiment. [e]While the literature-reported formula[S11,12] was

$Zr_6(OH)_4O_4(BzOH)_{12}(^nPrOH)$•4BzOH, we did not observe a significant amount of ^{n}PrOH and found much less BzOH than expected. We expected that our modified synthesis could have resulted in a loss of BzOH.

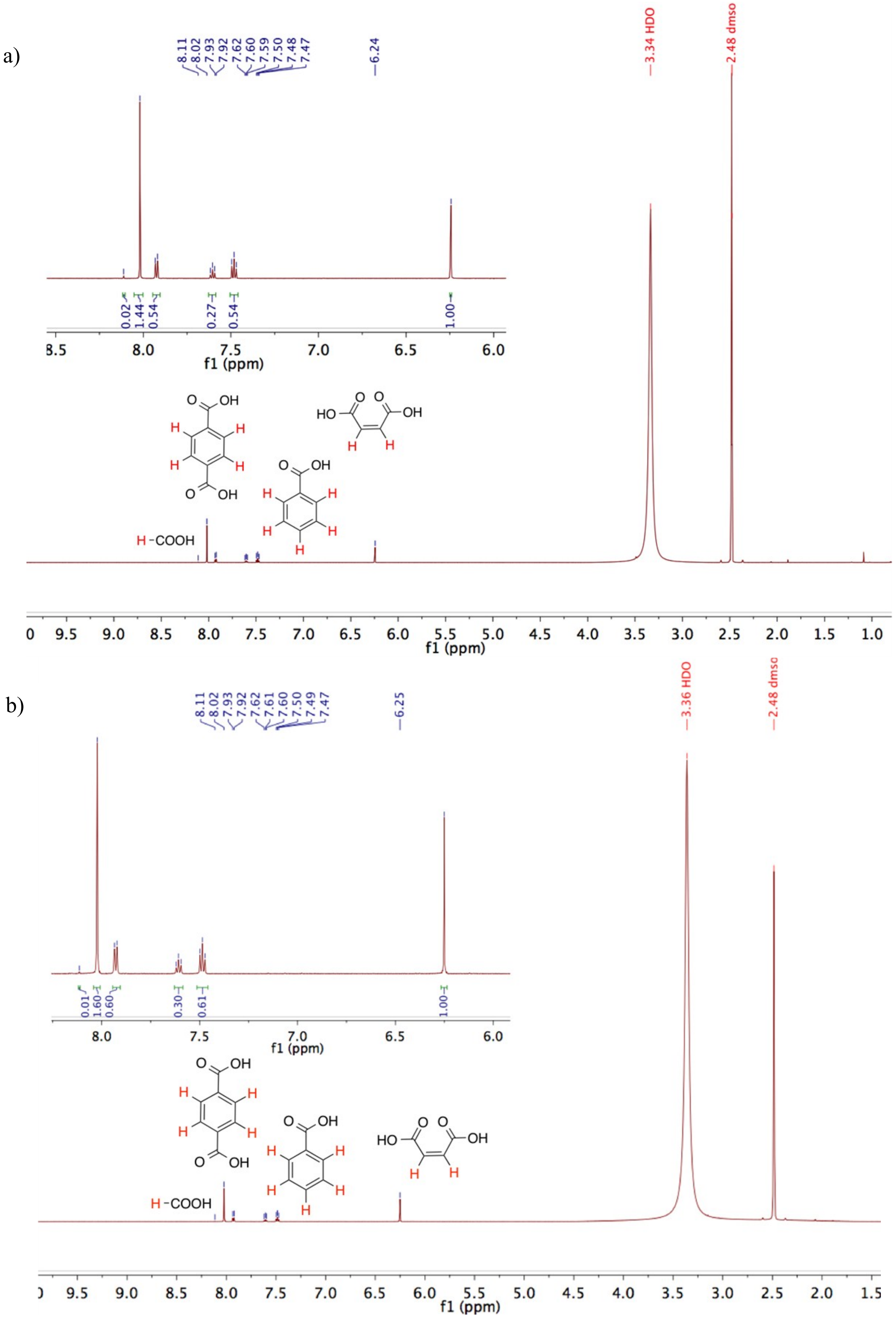

Figure S2. The ^{1}H NMR spectra of: a) digested **BzOH-UiO-66** batch 1 and b) digested **BzOH-UiO-66** batch 2 in DMSO-d_6.

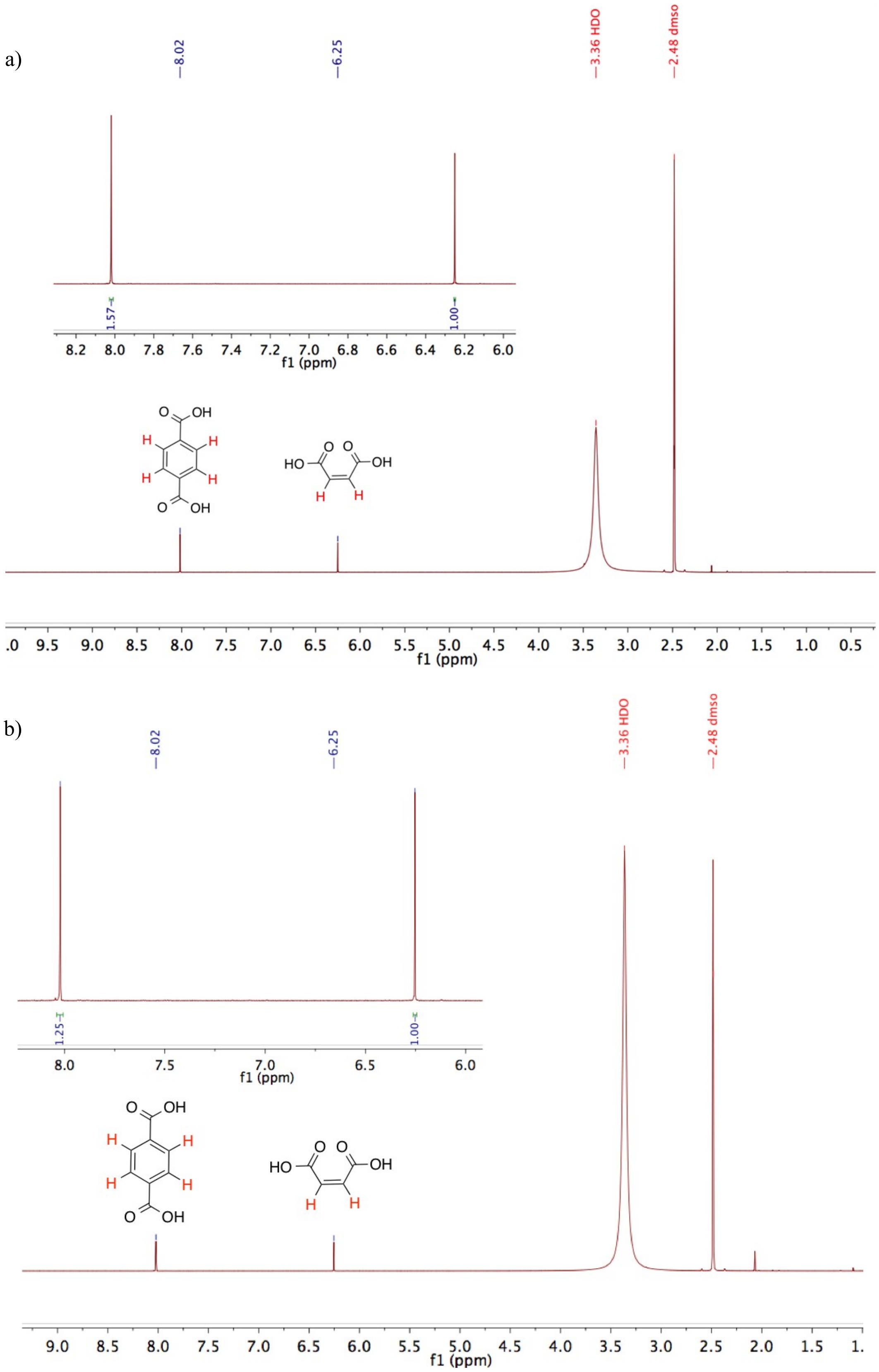

Figure S3. The ^{1}H NMR spectrum of: a) digested **decap-UiO-66** batch 1 and b) digested **decap-UiO-66** batch 2 in DMSO-d_6.

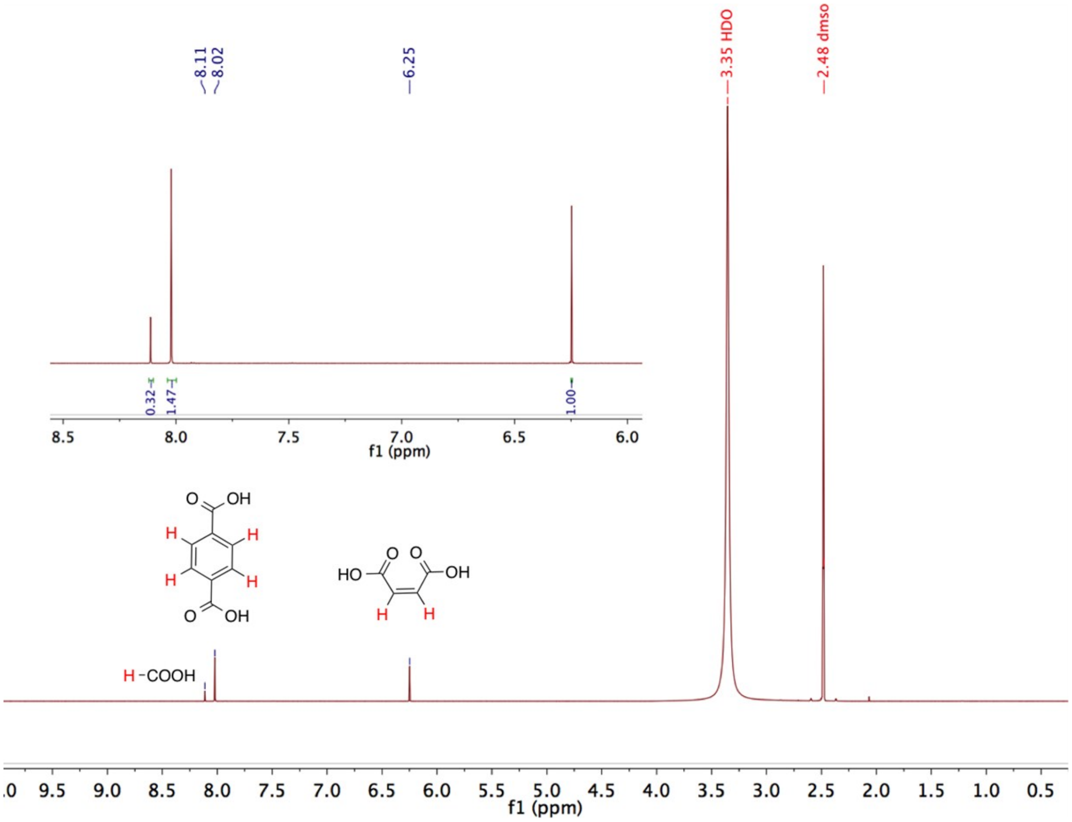

Figure S4. The ^{1}H NMR spectrum of digested **HCOOH-UiO-66** in DMSO-d_6.

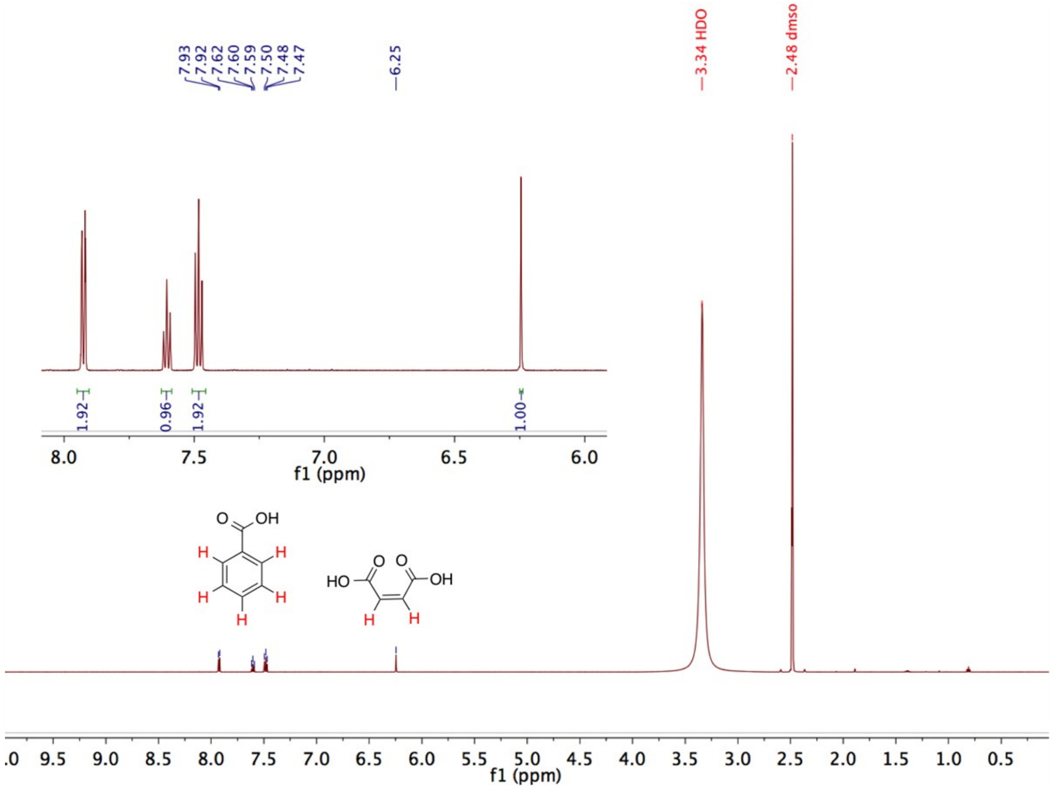

Figure S5. The ^{1}H NMR spectrum of digested **isolated Zr$_6$-oxo-hydroxo cluster** in DMSO-d_6.

S5. Characterization data of the MOF materials

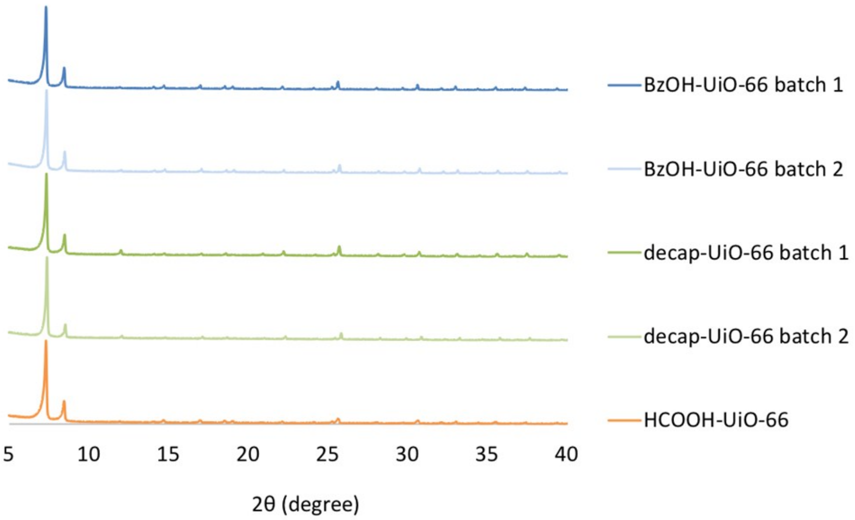

Figure S6. PXRD patterns for UiO-66 MOFs used in this study.

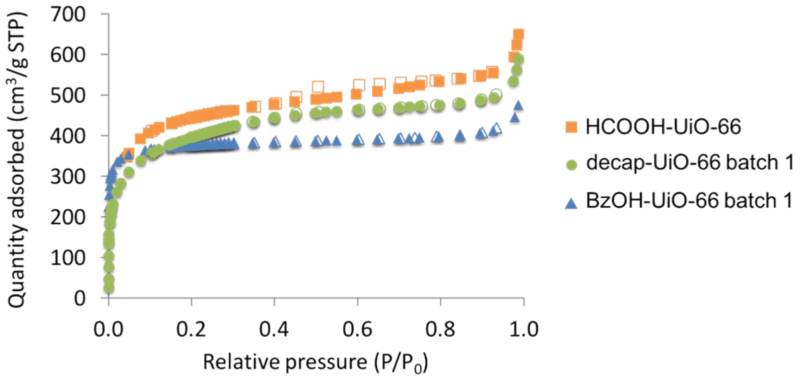

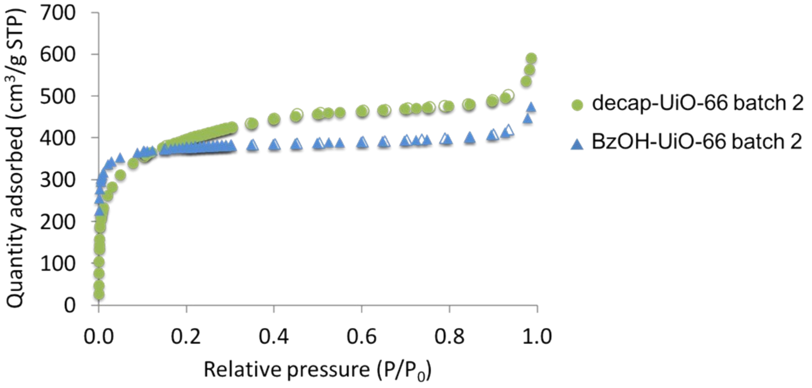

Figure S7. N_2 isotherms for UiO-66 MOFs used in this study: Close symbols: adsorption; open symbols: desorption.

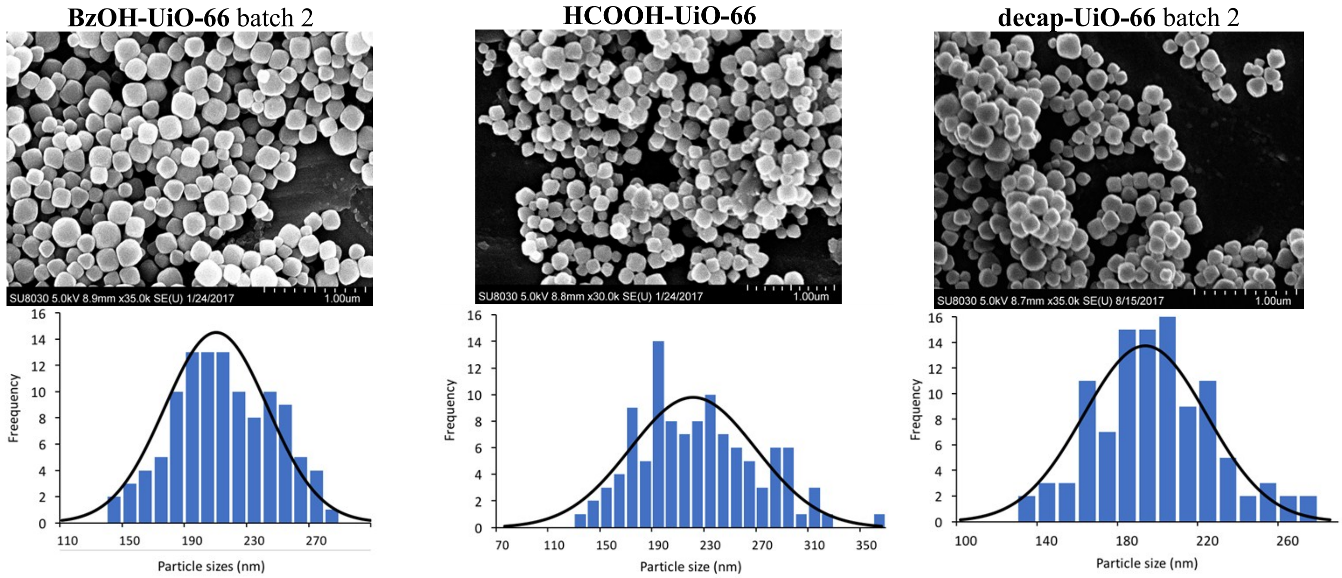
BzOH-UiO-66 batch 2

HCOOH-UiO-66

decap-UiO-66 batch 2

Figure S8. Top row: Representative SEM images of three UiO-66 MOFs used in this study. Bottom row: The corresponding SEM-derived particle-size-distribution profile for each of the MOF samples; each profile was constructed based on measurements of >100 particles.

S6. Procedures for the catalysis studies

Stock solution of 20 mM methyl phenyl sulfide or 20 mM methyl phenyl sulfoxide. In a 120 mL jar equipped with a magnetic stir bar, substrate (either methyl phenyl sulfide (240 µL, 2 mmol), or methyl phelnyl sulfoxide (280 mg, 2 mmol)), and naphthalene (256 mg, 2 mmol, as an internal standard) were dissolved in a selected solvent (either CH_3OH, CH_3CN, or CH_2Cl_2, 100 mL). This solution was stored at room temperature in a jar until use.

The oxidation of methyl phenyl sulfide with H_2O_2. These experiments were carried out with either **BzOH-UiO-66** batch 1 or **decap-UiO-66** batch 1. In a 6 dram vial equipped with a magnetic stir bar, a catalyst sample (0.012 mmol Zr (see Table S2), 6 mol %) was added to an aliquot of the pre-prepared 20 mM methyl phenyl sulfide stock solution (10 mL, 0.2 mmol). H_2O_2 (20 µL of a 30 wt % solution in water, 0.2 mmol) was then added and the mixture was stirred at room temperature. At specific time intervals (10 min or 1 h), an aliquot (0.3 mL) of the reaction mixture was removed and filtered through a 0.2 µm PTFE syringe filter (VWR International, North American Cat. No. 28145-495), that is attached to a disposable syringe. The filter was rinsed with additional reaction solvent (~1 mL) and the combined organics was then analyzed by GC-FID. Data are shown in Fig.1 and Table 2 in the manuscript, as well as Figures S9, S12-14. The error bars are the standard deviations of three trials.

Table S2. Catalysts used in the reaction.

Component	Amount of material[a] (mg)
decap-UiO-66	2.8
BzOH-UiO-66	3.4
HCOOH-UiO-66	2.9
Isolated Zr_6-oxo-hydroxo cluster	4.1
ZrO_2	1.2

[a] Calculated for a stoichiometry of 100 equiv substrate/$Zr_6O_4(OH)_4$ cluster based on the formula shown in Table S1.

The oxidation of methyl phenyl sulfoxide with H_2O_2. This reaction was conducted following the aforementioned procedure and with either **BzOH-UiO-66** batch 1 or **decap-UiO-66** batch 1. However, the pre-prepared 20 mM methyl phenyl sulfoxide stock solution was used as the substrate. Data are shown in Fig. 3 and Table 2 in the manuscript and Figure S10. The error bars are the standard deviations of three trials.

Catalyst recycling. These experiments were carried out with either **BzOH-UiO-66** batch 2 or **decap-UiO-66** batch 2. To reduce the proportion of catalyst loss during the recovery process, we carried out this series of experiments using an initial reaction scale that is 10 × larger than our typical catalysis experiment. Into a 250 mL round-bottom flask equipped with a magnetic stir bar, the appropriate MOF (0.1 mmol Zr, 5 mol%) or was added to a portion of the 20 mM methyl phenyl sulfide stock solution in methanol (100 mL, 2 mmol). H_2O_2 (200 µL of a 30 wt % solution in water, 2 mmol) was then added and the combined mixture was stirred at room temperature. At every 10 min, an aliquot (0.3 mL) of the reaction mixture was removed and filtered through a 0.2 µm PTFE syringe filter (VWR International, North American Cat. No. 28145-495), that is attached to a disposable syringe. The filter was rinsed with additional methanol (~1 mL) and the combined organics was then analyzed by GC-FID. After 90 min, the reaction mixture was subjected to centrifugation and the supernatant portion was isolated by carefully decanting to leave the catalyst behind. The remaining catalyst was immersed in fresh methanol (~15 mL) for ~5 min before being collected by centrifugation and decantation. This immersion and centrifugation process was repeated two more times. New aliquots of substrates and oxidant (same stoichiometry as shown above) were then added to repeat the oxidation of methyl phenyl sulfide. Data are shown in Figures S16-S19.

The PXRD of the catalysts after each cycles are shown in Figures S20-S21. The SEM data are shown in Figure S22.

To analyze the amount of Zr leaching, a portion (2 mL) of the clear supernatant collected at the end of each cycle was added to an 8 dram vial, and heated at 120 °C for 18 h to evaporate solvent and chemical substrates. Conc. H_2SO_4 (750 µL) and H_2O_2 (125 µL) were then added, and the vial was swirled briefly before the mixture was left unstirred at room temperature. After ~2 h (until the mixture became clear), the resulting clear solution was transferred to a 15 mL polypropylene centrifuge tube, and diluted with DI water to reach a final volume of 15 mL. The Zr content of this solution was then analyzed by ICP-OES (λ = 339.198, 343.823, 327.305, and 349.621 nm) comparing against a calibration curve of standards with known [Zr] concentrations. Data are listed in Table S3.

S7. Catalysis data. Unless otherwise noted in the caption, the materials employed in the experiments decribed below were from **BzOH-UiO-66** batch 1.

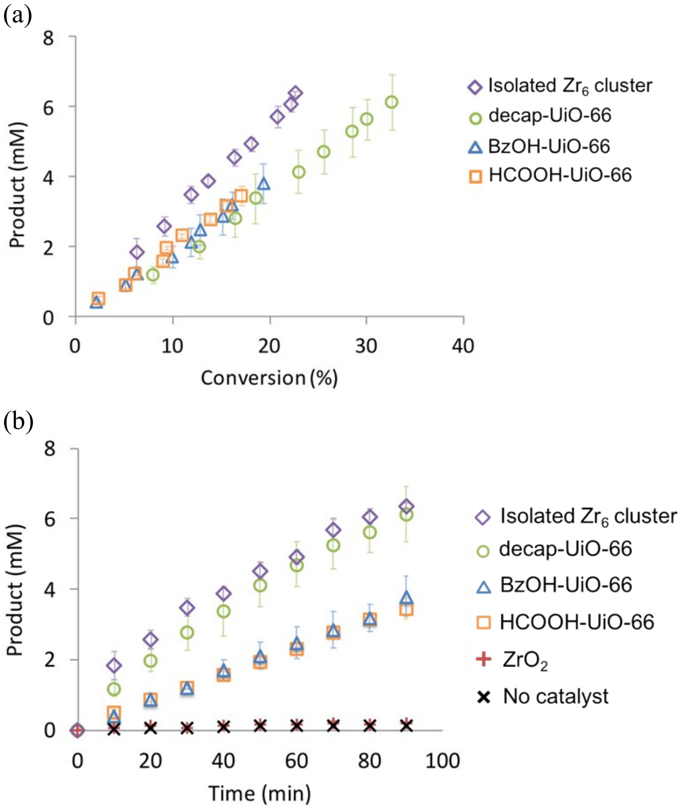

Figure S9. Product-formation profiles (product vs. conversion (a) and product vs. time (b)) in the catalytic oxidation of methyl phenyl sulfide in CH_3OH using H_2O_2 (1 equiv) as the oxidant. For convenience, product = sulfoxide + sulfone

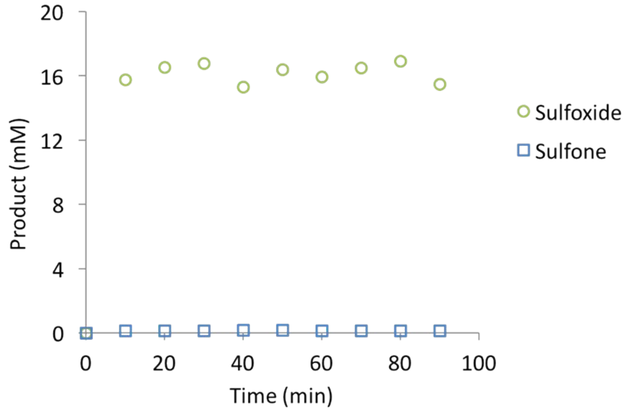

Figure S11. Product-formation profiles in the uncatalyzed oxidation of methyl phenyl sulfide in CH_3OH using BzOOH (~0.8 equiv) as an oxidant.

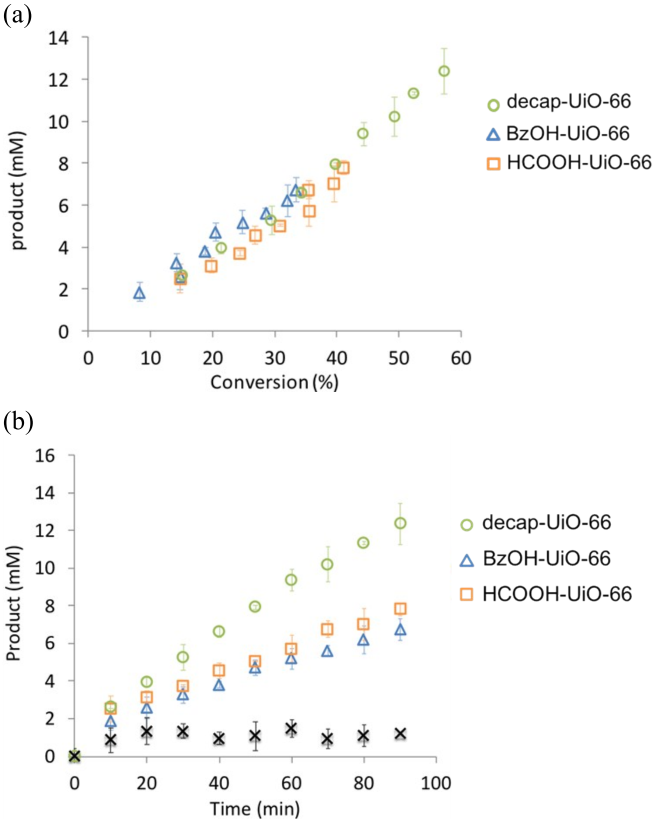

Figure S10. Product-formation profiles (product vs. conversion (a) and product vs. time (b)) in the catalytic oxidation of methyl phenyl sulfoxide in CH_3OH using H_2O_2 (1 equiv) as the oxidant.

Because carboxylic acids can potentially be converted to peracids after treating with H_2O_2 under acidic condition,[S13] we initially suspected that BzOOH might form on the Zr_6-oxo-hydroxo cluster nodes of **BzOH-UiO-66**, and provide an additional pathway for oxidizing the sulfide. Thus, we carried out the uncatalyzed oxidation of methyl phenyl sulfide using BzOOH oxidant (Figure S11) as a control. However, this experiment does not result in sulfone (~99% selectivity to sulfoxide), which was very different from our observed sulfide reaction in the presence of **BzOH-UiO-66** and H_2O_2, where the sulfoxide selectivity was only ~70% (Fig. 1b in the manuscript). In addition, DFT calculations reveal a barrier of 164 kJ/mol for the catalyst activation step, which is much higher than all of the barriers in the favored Zr-μ_1-OOH mechanism (Fig. 2 in the manuscript). Together, these data suggest that the formation of BzOOH is less likely to occur under our reaction conditions.

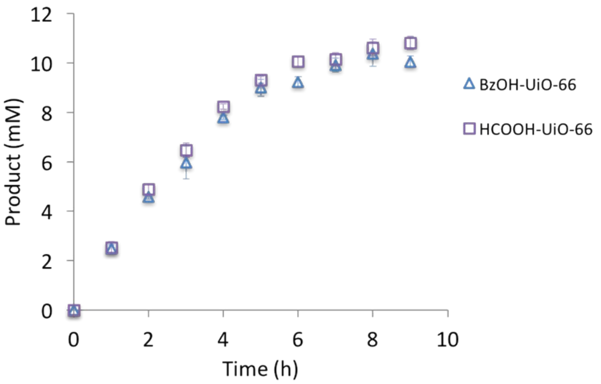

Figure S12. Product-formation profiles (9 h, product vs. time) in the catalytic oxidation of methyl phenyl sulfide in CH_3OH using H_2O_2 (1 equiv) as the oxidant. For convenience, product = sulfoxide + sulfone

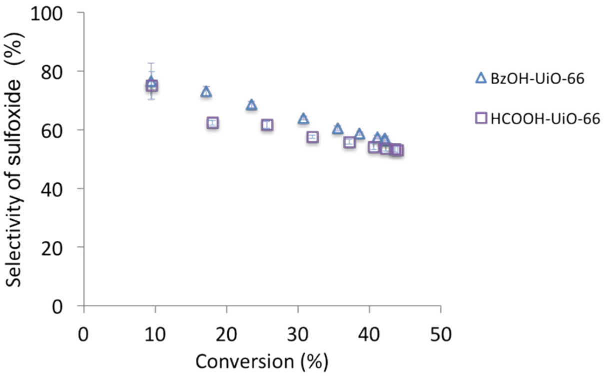

Figure S14. Selectivity profiles (9 h) in the catalytic oxidation of methyl phenyl sulfide in CH_3OH using H_2O_2 (1 equiv) as the oxidant.

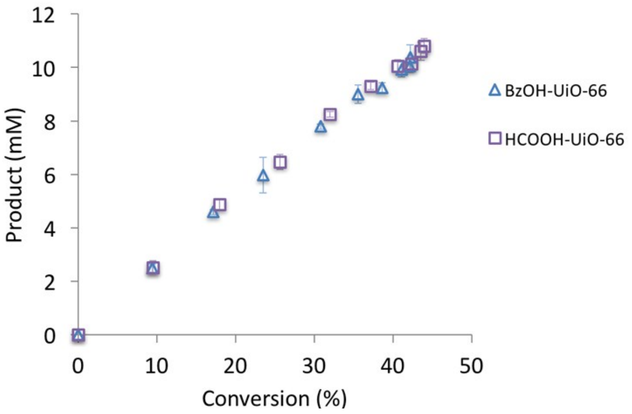

Figure S13. Product-formation profiles (9 h, product vs. conversion) in the catalytic oxidation of methyl phenyl sulfide in CH_3OH using H_2O_2 (1 equiv) as the oxidant. For convenience, product = sulfoxide + sulfone

Figures S16-S19 below show the recycling data for **BzOH-UiO-66** batch 2 and **decap-UiO-66** batch 2 in the catalytic oxidation of methyl phenyl sulfide in CH_3OH using H_2O_2 as the oxidant. In comparison to the respective data in Fig. 1a in the manuscript, the product-formation profiles for these materials are slightly slower. However, the sulfide selectivity trends (cf Figure S17 and S19 vs Fig. 1b in the manuscript) are very similar. In addition, the difference in initial rate of sulfide oxidation between **BzOH-UiO-66** batch 2 and **decap-UiO-66** batch 2 (6.5×10^{-7} and 10.0×10^{-7} M/s, respectively) follow the same trend as shown in Table 2 in the manuscript, with the latter material approximatelly twice as fast as the former. Together with the near-indistinguishable characterization data reported for both batches, these data accentuate a main point of our work that subtle variations in MOF starting materials can lead to differences in catalysis results; however, a systematic comparison is best made with materials derived from the same source.

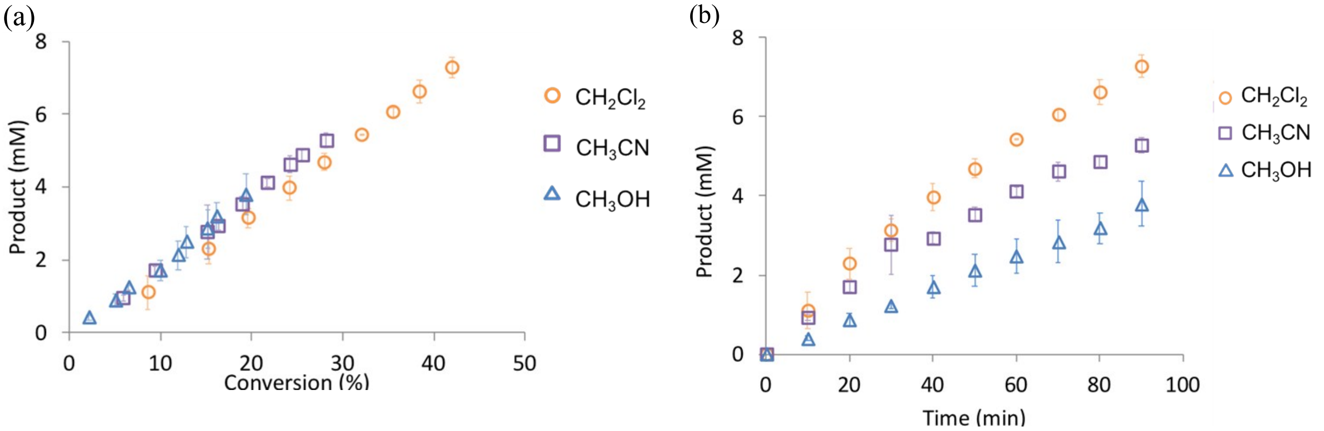

Figure S15. Product-formation profiles (product vs. conversion (a) and product vs. time (b)) in the catalytic oxidation of methyl phenyl sulfide using H_2O_2 as the oxidant and **BzOH-UiO-66** as the catalyst in three different solvents. For convenience, product = sulfoxide + sulfone

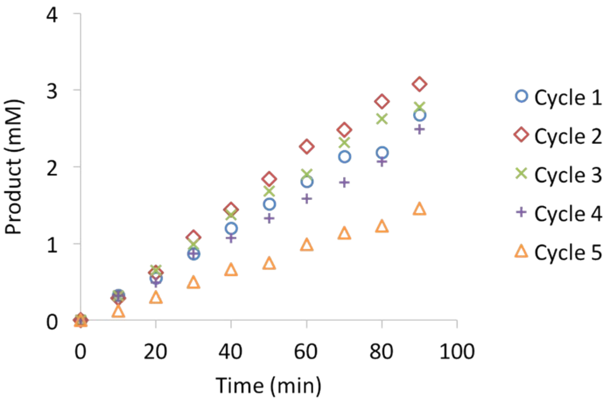

Figure S16. Product-formation profiles in the catalytic oxidation of methyl phenyl sulfide in CH_3OH using H_2O_2 (1 equiv) as the oxidant and **BzOH-UiO-66** batch 2 as the catalyst. Five cycles were carried out. For convenience, product = sulfoxide + sulfone.

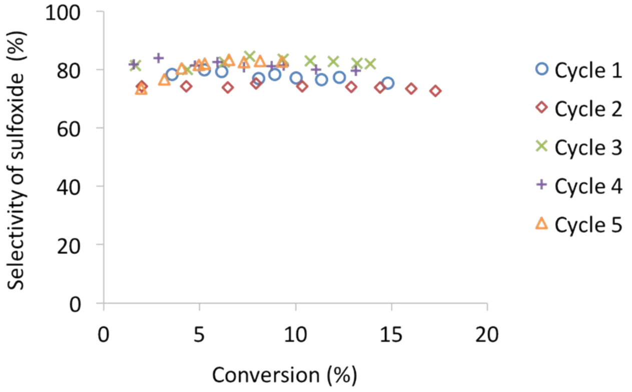

Figure S17. Selectivity profiles in the catalytic oxidation of methyl phenyl sulfide in CH_3OH using H_2O_2 (1 equiv) as the oxidant and **BzOH-UiO-66** batch 2 as the catalyst. Five cycles were carried out.

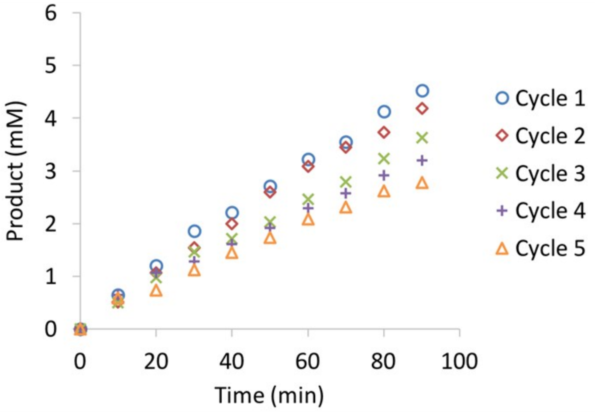

Figure S18. Product-formation profiles in the catalytic oxidation of methyl phenyl sulfide in CH_3OH using H_2O_2 (1 equiv) as the oxidant and **decap-UiO-66** as the catalyst. The materials used in this study came from **BzOH-UiO-66** batch 2. Five cycles were carried out. For convenience, product = sulfoxide + sulfone.

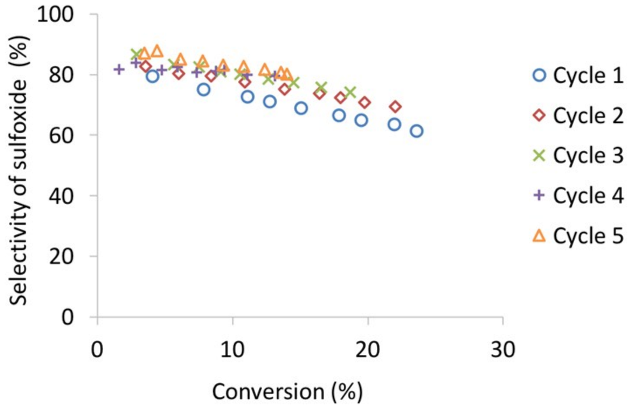

Figure S19. Selectivity profiles in the catalytic oxidation of methyl phenyl sulfide in CH_3OH using H_2O_2 (1 equiv) as the oxidant and **decap-UiO-66** as the catalyst. The materials used in this study came from **BzOH-UiO-66** batch 2. Five cycles were carried out.

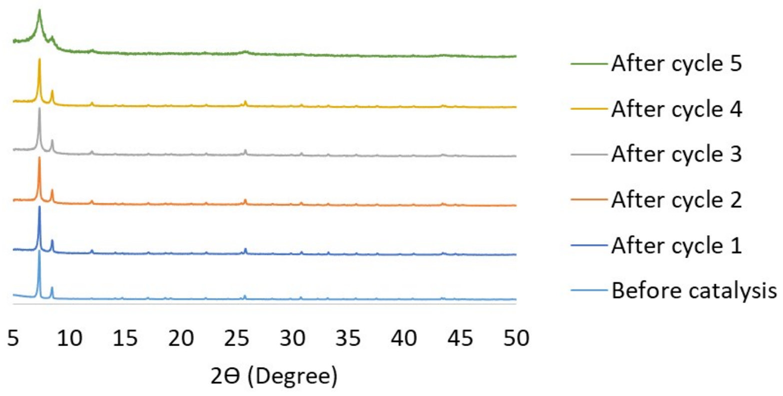

Figure S20. PXRD patterns for **BzOH-UiO-66** batch 2 before and after catalysis.

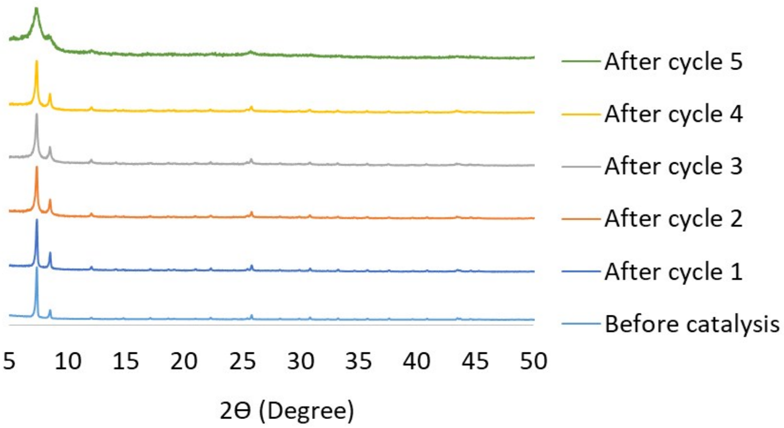

Figure S21. PXRD patterns for **decap-UiO-66** batch 2 before and after catalysis.

BzOH-UiO-66 after cycle 4 **decap-UiO-66** after cycle 4

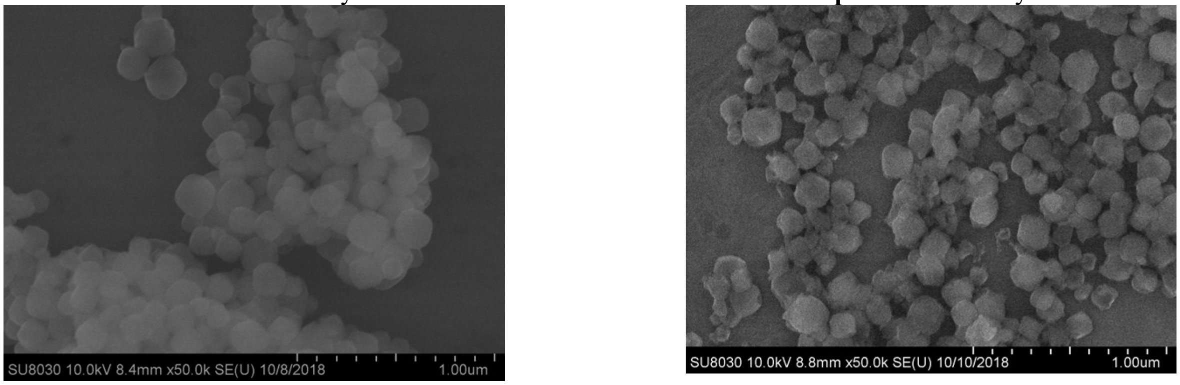

BzOH-UiO-66 after cycle 5 **decap-UiO-66** after cycle 5

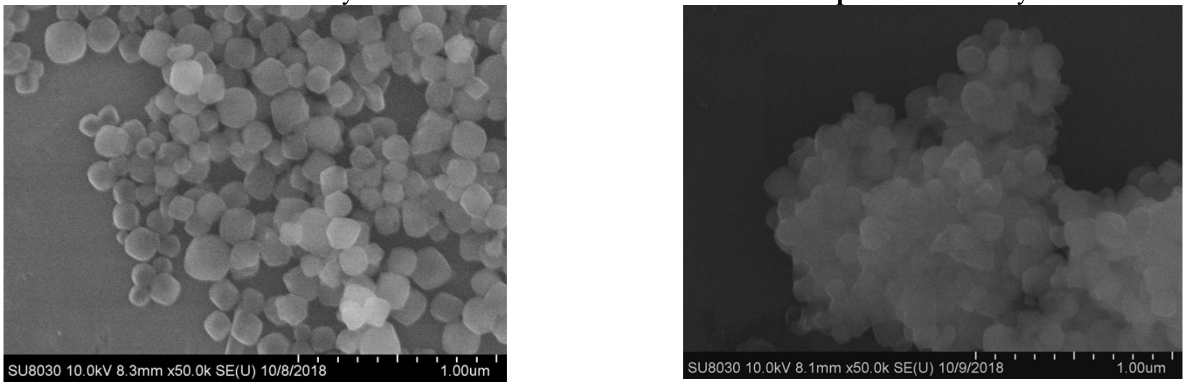

Figure S22. SEM images of UiO-66 MOFs after cycles 4 (top panels) and 5 (bottom panels) of catalysis. While there is no visible changes in morphology, the broadening of the PXRD profiles shown in Figures S20-21 suggest some loss of crystallinity.

Table S3. Amount of Zr leached out into solution after each cycle.

Cycle	**Amount of Zr in supernatant (mg)**[a]	
	decap-UiO-66	**BzOH-UiO-66**
1	0.010	0.156
2	0.002	0.038
3	0.008	0.013
4	0.013	0.006
5	0.013	0.004

[a] The values reported are calculated from ICP-OES analyses against a calibration curve and are based only one run for each sample. Thus, the number of significant figures should not be taken literally. The total amount of leached Zr after the 5th cycle is less than 1 wt % of the initial catalyst amount.

S8. Additional computational data

Table S4. Relative enthalpy values (ΔH, kJ/mol) for the various species in the oxidation of methyl phenyl sulfide without catalyst (corresponding to the "Uncatalyzed" profile in Fig. 2 in the manuscript).

Reactant	**TS for the 1st oxidation**	**Intermediate**	**TS for the 2nd oxidation**	**Product**
0.0	62.7	-214.3	-131.5	-518.8

Table S5. Relative enthalpy values (ΔH, kJ/mol) for the various species in the oxidation of methyl phenyl sulfide by the Zr_6-oxo-hydroxo cluster node of UiO-66 (corresponding to the "Node of UiO-66" profile in Fig. 2 in the manuscript)

Reactant	**TS for the catalyst activation**	**Active catalyst**	**TS for the 1st oxidation**	**Intermediate**	**TS for the catalyst activation**	**Active catalyst**	**TS for the 2nd Oxidation**	**Product**
0.0	25.6	-4.0	7.8	-214.3	-188.3	-217.9	-165.8	-518.8

Table S6. Binding enthalpies of three different solvents and substrates to the Zr_6-oxo-hydroxo cluster node of UiO-66.

Solvent/substrate	**ΔH_{bind} (kJ/mol)**
H_2O	-88.0
CH_3OH	-88.0
CH_3CN	-47.5
CH_2Cl_2	-32.8
Methyl phenyl sulfide	No binding
Methyl phenyl sulfoxide	-87.6
Methyl phenyl sulfone	-71.7

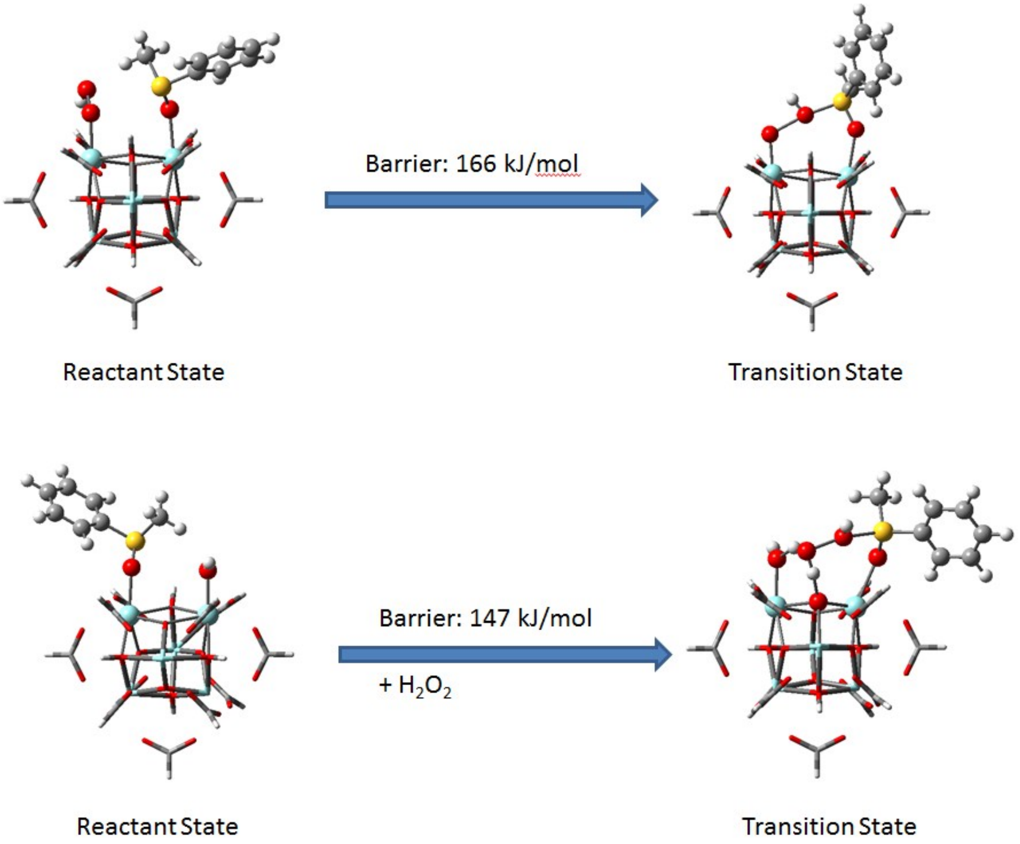

Figure S23. Two possible Langmuir-Hinshelwood type reaction mechanisms of sulfoxide oxidation obtained from DFT calculations.

As discussed in footnote 62 in the manuscript, we searched for a Zr(η^2-O_2) intermediate that was proposed to form in the presence of H_2O_2.[S17] However, such a species does not appear to be a stable intermediate: in our DFT calculations, the 3-member Zr(η^2-O_2) peroxy ring breaks during the optimization and forms a Zr-μ_1-OOH species (Figure S24) that is 58 kJ/mol higher in energy than the Zr-μ_1-OOH species shown in Fig. 2 of the manuscript. Thus, we proceeded with the lower-energy structure.

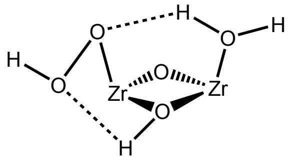

Active catalyst structure (Zr-μ_1-OOH) in Fig. 2 of the manuscript.
E = 0 kJ/mol

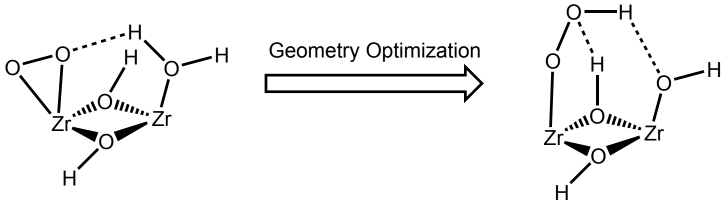

Proposed alternative structure (Zr(O_2))

Optimized alternative structure, Zr(O_2) motif is broken up.
E = +58 kJ/mol

Figure S24. Top: A structural drawing of the Zr-μ_1-OOH species shown in Fig. 2 of the manuscript. Bottom: Outcome of an attempt to carry out geometry optimization of the 3-member Zr(η^2-O_2) peroxy ring proposed by Faccioli et al.[S17]

S9. Optimized structures and Cartesian coordinates of key species

White, grey, red, yellow, and cyan spheres represent H, C, O, S, and Zr atoms, respectively. Active site and the reagent atoms are shown in the "ball and stick" format while the other atoms are shown in the "tube" format.

Uncatalyzed pathway

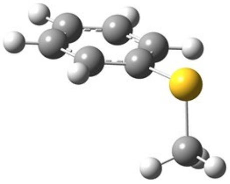

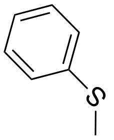

$C_6H_5SCH_3$

C	1.94711600	-1.21104700	0.10842200
C	0.57149400	-1.21297500	-0.14450600
C	-0.12490900	0.00000000	-0.26649900
C	0.57149400	1.21297500	-0.14450700
C	1.94711600	1.21104700	0.10842200
C	2.63649800	0.00000000	0.23510000
H	2.48205900	-2.15956800	0.20292900
H	0.03071400	-2.15643300	-0.24999900
H	0.03071400	2.15643300	-0.25000000
H	2.48205900	2.15956800	0.20292800
H	3.71191800	0.00000000	0.42998000
S	-1.88429300	0.00000000	-0.63507100
C	-2.59860600	0.00000100	1.05156500
H	-2.29945600	0.90065800	1.60643500
H	-3.69107900	-0.00000100	0.92444900
H	-2.29945600	-0.90065600	1.60643600

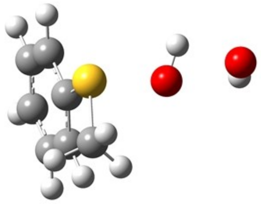

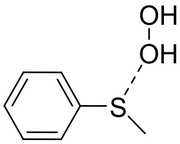

TS for the 1st oxidation $C_6H_5SCH_3 + H_2O_2$

O	-2.20964200	0.52240400	0.10461400
O	-3.40602200	2.06200900	0.58911800
H	-2.42712600	1.22438500	-0.54463100
H	-2.70752000	2.42044000	1.15928000
S	-0.99239000	-0.80529600	-0.81915200
H	-0.77694700	-2.92893100	0.30684200
C	-1.48831100	-2.09338700	0.34205700
H	-1.56994000	-1.67099400	1.35144100
H	-2.47818500	-2.42419000	0.00274700
C	0.61879200	-0.29680700	-0.28060900
C	1.37328400	0.43524200	-1.21508600
C	1.13521700	-0.55328500	0.99930600
C	2.63761500	0.91030400	-0.86452100
H	0.97216000	0.62746300	-2.21330500
C	2.40629700	-0.07880000	1.33358300
H	0.56356600	-1.11726300	1.73677000
C	3.15841800	0.65372200	0.40904800
H	3.22049800	1.47809900	-1.59350100
H	2.80863200	-0.28365400	2.32851800
H	4.15054000	1.02212700	0.67974000

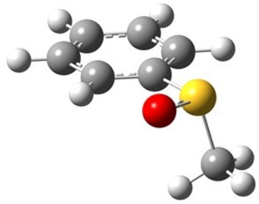

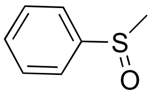

$C_6H_5S(O)CH_3$

C	-2.07130500	1.23746100	0.36331200
C	-0.68690400	1.14877500	0.18225100
C	-0.12782400	-0.07561500	-0.18396700
C	-0.92238300	-1.20574300	-0.40371100
C	-2.30465100	-1.10798000	-0.21602600
C	-2.87812400	0.11099700	0.16746000
H	-2.52128600	2.19007300	0.65432700
H	-0.02802000	2.01043200	0.31339500
H	-0.47491600	-2.15293900	-0.71802900
H	-2.93678000	-1.98457300	-0.37790800
H	-3.95959100	0.18345000	0.30648000
C	2.14220400	-0.95050300	1.10351800
H	1.69997900	-1.95542700	1.15233300
H	3.23920300	-1.01462600	1.09837000
H	1.79317700	-0.31577900	1.92965800
S	1.67492600	-0.13897500	-0.47286300
O	2.18541800	1.28983000	-0.35872900

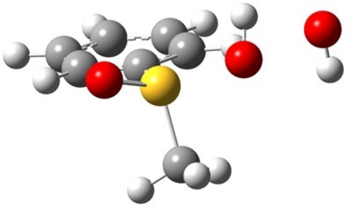

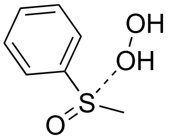

TS for the 2nd oxidation $C_6H_5S(O)CH_3 + H_2O_2$

O	-2.07676200	0.71012400	-0.33444600
H	-1.77230100	1.17598700	-1.13503600
O	-0.96367300	-2.26269100	-0.84774100
S	-1.06000300	-0.92420300	-0.18298300
C	0.59605800	-0.21420800	-0.05386600
C	0.77382000	1.16377100	0.13179800
C	1.67523800	-1.09424400	-0.18862200
C	2.08044300	1.65389000	0.21368500
H	-0.08422200	1.83953200	0.18107600
C	2.97209700	-0.58241700	-0.10277300
H	1.49548100	-2.15693600	-0.36151100
C	3.17386000	0.78717200	0.10259500
H	2.24259100	2.72464000	0.35728600
H	3.82640400	-1.25618600	-0.19998300
H	4.19002300	1.18334900	0.16660600
C	-1.58239100	-1.18498800	1.52574900
H	-1.50505600	-0.23837500	2.07223700
H	-2.62367800	-1.53120200	1.47824500
H	-0.92933200	-1.95966800	1.94747600
O	-2.41460600	2.69752000	-0.31781300
H	-2.37428700	2.67262800	0.64994000

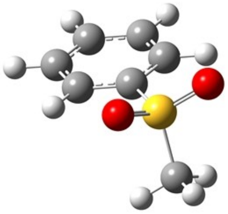

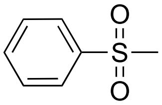

$C_6H_5S(O)(O)CH_3$

C	-2.40436500	1.21464600	0.04047700
C	-1.00877900	1.22180800	-0.03144800
C	-0.32896500	0.00000900	-0.05824100
C	-1.00875900	-1.22179700	-0.03153100
C	-2.40434000	-1.21467600	0.04038600
C	-3.09896600	-0.00002400	0.07837200
H	-2.95058900	2.16047900	0.06085900
H	-0.45096100	2.15879300	-0.07731500
H	-0.45085000	-2.15873200	-0.07743100
H	-2.95055700	-2.16051600	0.06065400
H	-4.19027900	-0.00004400	0.13234200
C	2.04685600	-0.00049400	1.53933300
H	1.68753900	-0.90790700	2.04064700
H	3.14386800	-0.00113500	1.47102500
H	1.68860900	0.90728600	2.04075400
S	1.46803200	0.00004800	-0.16461400
O	1.88930100	1.27378500	-0.77967700
O	1.88927600	-1.27326200	-0.78054800

Catalyzed pathway

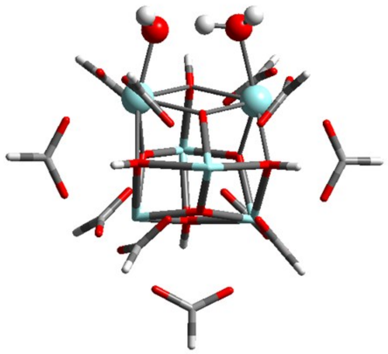

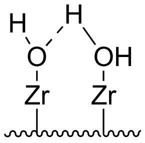

Initial state ($[Zr_6(\mu_3\text{-}O)_4(\mu_3\text{-}OH)_4(\mu_1\text{-}OH)(\mu_1\text{-}OH_2)(HCOO)_{11}]$)

C	1.98712600	3.04378900	-2.68945700
C	4.48626600	0.24217400	-0.48905700
C	2.05735300	-3.30982900	-2.32892600
C	2.40190600	3.43748900	1.61001700
C	0.44787900	0.28246900	4.44592900
C	-2.27802500	-3.48779800	-1.82822000
C	-4.50016500	-0.05706600	0.42550300
C	2.54395900	-2.89138800	2.32664200
C	-2.69562200	2.93196000	-2.15191100
C	-1.80164100	-3.01885700	2.77277900
C	-2.22479300	3.29629500	2.08070600
O	-1.72153900	-0.39090600	-3.75359800
O	1.16821000	3.48736600	-1.84141900
O	2.26256800	1.83628900	-2.91727100
O	2.28690400	-2.12952800	-2.72081800
O	3.82419600	0.07255200	-1.54541900
O	2.05072700	-1.34865600	-0.12172900
O	-0.26410600	1.19570400	-2.18588900
O	1.42374300	1.08070000	-0.27120700
O	-0.10152800	-1.17901900	-1.41299800
O	4.03347800	0.28526300	0.68546700
O	1.37876200	-3.66014800	-1.32993100
O	0.14787300	1.58659200	1.83226200
O	2.82817900	-1.66862900	2.44420100
O	2.72975100	2.28459300	2.00254000
O	1.51390600	0.32300200	3.77509000
O	0.19795800	-0.90603300	1.51501000
O	-1.92680900	-1.47455400	0.28622800
O	-2.97544000	1.71825200	-2.29514600
O	-2.67942500	-2.34286500	-2.16523100
O	-4.06011800	-0.21064900	-0.74288600
O	-1.48988600	0.99265900	0.02175900
O	-1.05840400	-3.46943800	1.86106000
O	1.67425300	-3.39732200	1.57127200
O	-1.35713700	-3.76016900	-1.01202600
O	-1.44607300	3.65527200	1.15762500
O	-1.69721900	3.41489300	-1.54753700
O	1.43758700	3.73595500	0.85909200
O	-0.72698900	0.24219800	3.99661100
O	-3.82166200	0.05014900	1.48034900
O	-2.15525300	-1.82112800	2.94068300
O	-2.39811000	2.12639800	2.51562000
Zr	1.60212500	-0.10311600	-1.97158900
Zr	-1.98771300	-0.23187200	-1.65505600
Zr	-0.10773300	2.51140800	-0.25786100
Zr	1.96476100	0.21873300	1.56857000
Zr	0.10533000	-2.51158400	0.17410200
Zr	-1.59582000	0.10781700	1.91037200
H	-0.37372600	1.67101400	-3.02218100
H	2.85461700	-1.88483500	-0.15421700
H	0.20383500	2.21195100	2.56729700
H	-2.68091900	-2.06181000	0.43035000
O	0.79396800	-0.36367300	-4.10932200
H	-0.24418900	-0.40444000	-4.07642400
H	5.58467200	0.35733600	-0.60215600
H	3.13187900	-3.59679900	2.95099800
H	0.55793100	0.29137400	5.55068300
H	-2.81678000	4.09844900	2.56938800
H	-5.60423000	-0.02056000	0.54044800
H	-2.19524900	-3.75826300	3.50165200
H	2.51207800	-4.12320400	-2.93235600
H	2.51783000	3.79848500	-3.30724600
H	-2.79546300	-4.35244800	-2.29487900
H	3.02844000	4.27884200	1.97371900
H	-3.39293200	3.66527900	-2.61006500
H	-2.14927400	-1.17185000	-4.13583300
H	1.09910100	-1.19041000	-4.51426500

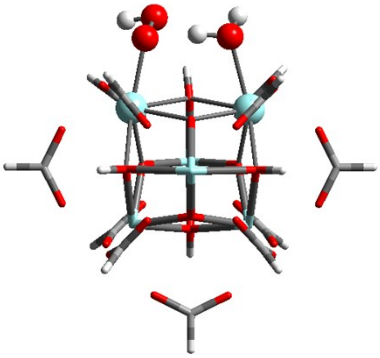

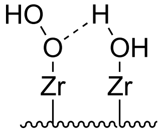

Active catalyst ($[Zr_6(\mu_3\text{-}O)_4(\mu_3\text{-}OH)_4(\mu_1\text{-}OOH)(\mu_1\text{-}OH_2)(HCOO)_{11}]$)

C	-2.13731400	3.86465800	0.72967200
C	2.06687100	3.99858800	-0.43334100
C	1.04524500	1.41515500	-4.17157100
C	1.02947400	2.61404100	3.52896700
C	3.35972500	-1.34518200	2.73488900
C	-1.03862800	-2.37018700	-3.68129700
C	-2.07203900	-3.94081500	0.61318100
C	4.37751400	0.02319000	-1.27533000
C	-4.22818400	-0.28275400	1.48745400
C	2.36789800	-3.78994700	-0.72005000
C	-1.09865000	-1.48591700	4.08658000
O	-3.50697400	-0.02992600	-2.20445200
O	-2.11503700	3.03913300	1.67870000
O	-1.63331500	3.72008400	-0.41938300
O	0.41894900	2.22712700	-3.44006000
O	1.01268800	3.82464700	-1.10083500
O	1.70669500	1.22285800	-1.32917000
O	-2.14434900	1.09511500	-0.19511400
O	0.18468000	1.68240500	0.61544400
O	-0.49489400	0.04679300	-1.76356300
O	2.65596100	3.14672400	0.28530500
O	1.48063800	0.27837500	-3.84296400
O	0.75904300	-0.04816600	2.33292900
O	4.10408600	0.67275600	-0.23078100
O	1.98981700	2.29144100	2.78241100
O	3.45536000	-0.16856300	2.28940000
O	1.64168500	-0.81781500	0.10903800
O	-0.14964300	-2.28603900	-0.86015800
O	-3.97825300	-0.89440100	0.41525500
O	-1.98277100	-2.11036200	-2.88832700
O	-2.60665500	-3.14195300	-0.20180300
O	-1.17374800	-0.90056100	0.98694800
O	2.31234000	-2.97210600	-1.67751600
O	3.56693400	-0.56932200	-2.03817400
O	0.18271500	-2.11385400	-3.51560400
O	-1.48961500	-0.32735900	3.78310000
O	-3.44970200	0.47604700	2.12223300
O	-0.16620500	2.23014700	3.43124400
O	2.41252100	-2.15189500	2.54508100
O	-0.98614800	-3.77934000	1.23174900
O	1.78755800	-3.69460400	0.39423500
O	-0.36638000	-2.24769900	3.39812900
Zr	-0.39501400	2.08089300	-1.33438700
Zr	-2.09870200	-1.06132600	-0.89531100
Zr	-1.27484600	0.95518900	1.93283600
Zr	2.16665800	1.04218900	0.90055900
Zr	1.34411300	-0.95250200	-1.96186300
Zr	0.50537100	-2.08780400	1.32816300
H	-3.04056700	1.44412600	-0.36996800
H	2.35681200	1.70761900	-1.85556200
H	1.03895900	-0.06780900	3.25819000
H	-0.21631300	-3.18890500	-1.19933700
O	-2.21635400	2.17593000	-2.77406400
H	-2.90033500	2.83668500	-2.58350800
H	-2.69089700	1.28529700	-2.76110100
H	2.53056700	5.00534700	-0.48935100
H	5.44923400	-0.02483700	-1.56148300
H	4.19808100	-1.70234600	3.36876200
H	-1.42781700	-1.87661700	5.07229400
H	-2.61168000	-4.89281400	0.79992700
H	2.98916400	-4.69614900	-0.87901500
H	1.24385200	1.73823100	-5.21486300
H	-2.65958600	4.82564300	0.91934600
H	-1.31240900	-2.88851700	-4.62431100
H	1.26181700	3.30276300	4.36827500
H	-5.24574000	-0.41441600	1.91167500
O	-4.44911400	0.88275800	-1.58118200
H	-4.99792400	0.26918000	-1.0592230

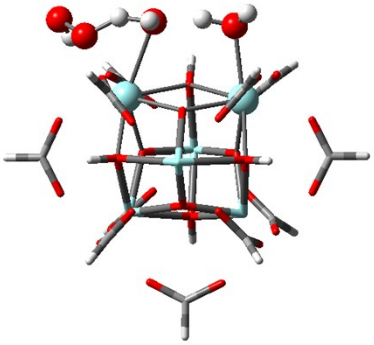

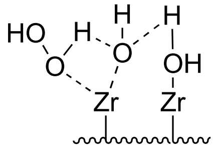

Catalyst activation TS ($[\mathrm{Zr_6}(\mu_3\text{-O})_4(\mu_3\text{-OH})_4(\mu_1\text{-OH})(\mu_1\text{-OH_2})(\mathrm{HCOO})_{11}] + \mathrm{H_2O_2}$)

C	-3.29075600	-2.77986300	-1.12473000	O	-0.07034200	-2.59347500	-3.15032100
C	-3.22095400	-0.92316900	2.90305500	O	-0.40516500	-4.05136800	0.49218700
C	-2.55770900	3.50259000	1.07582000	O	3.55641600	-1.10899800	1.96968200
C	-0.49851300	-4.11261200	1.74727300	O	3.80453000	0.23680400	-1.80207300
C	3.07620900	-1.46752400	3.07780700	O	3.89648200	1.36606900	0.87383400
C	0.54145500	4.12778500	-1.78032800	O	3.49489500	-2.22928000	-0.72167000
C	3.48531100	0.70607900	-2.92562500	Zr	-2.47147600	0.32995400	-0.02943100
C	0.39338400	1.72081800	4.13492600	Zr	0.30835500	0.92371800	-2.33508000
C	0.17679500	-1.81342800	-4.11026500	Zr	-0.14232700	-2.32410300	-0.93805100
C	3.62555700	2.50453200	1.34416100	Zr	-0.05141200	-0.94045900	2.33060700
C	2.98120700	-3.26811700	-1.22166600	Zr	0.40065400	2.31638600	0.92813700
O	-1.40067800	1.59778700	-3.73121800	Zr	2.65040400	-0.31346600	0.05702000
O	-2.13104700	-3.19587500	-1.37091900	H	-1.97942000	-0.80093300	-2.65740700
O	-3.59366100	-1.64198700	-0.68535300	H	-1.76001300	1.34250400	2.51824200
O	-3.11535500	2.47661100	0.61755300	H	1.73944500	-2.78898300	1.13266000
O	-3.55951400	-0.39396900	1.81456100	H	2.41885300	2.30680800	-1.05764800
O	-1.24824200	0.95712800	1.79340400	O	-3.30471100	1.69401600	-2.04932300
O	-1.43348600	-0.52332000	-1.90702300	H	-2.26006700	1.62578000	-3.18751300
O	-1.10706300	-1.20987100	0.53517300	H	-4.04130000	-1.19972900	3.59808600
O	-0.74582400	1.48206500	-0.61402400	H	0.53136500	2.13794200	5.15450000
O	-2.04800700	-1.16616200	3.29614800	H	3.80509100	-1.77056400	3.85856100
O	-1.32869300	3.65247800	1.32348600	H	3.68917700	-4.04906700	-1.56974900
O	1.28889900	-1.99691500	0.80970200	H	4.30406300	0.83233800	-3.66416000
O	0.16656200	0.48327700	4.05984300	H	4.48229700	3.09833900	1.72542800
O	-0.38109600	-3.15869600	2.56084800	H	-3.21002500	4.37505100	1.29267500
O	1.85848500	-1.52767700	3.39031300	H	-4.12617100	-3.48302500	-1.32382700
O	1.20025400	0.43896000	1.36671000	H	0.57600900	5.14538800	-2.22234000
O	1.77497000	1.64925800	-0.76125700	H	-0.69784500	-5.11443400	2.18172600
O	0.31789000	-0.56827700	-4.04591300	H	0.26928600	-2.27891800	-5.11383900
O	0.45697400	3.16606700	-2.59576000	H	-1.25963700	2.49987600	-4.06128700
O	2.33282800	1.05664000	-3.29608300	H	-3.28129200	2.61499600	-1.74460700
O	1.11052700	-0.70380600	-1.33194100	O	-4.68119400	0.73064900	-0.47364100
O	2.48925300	3.04040500	1.41659000	H	-4.22550300	1.25209400	-1.53058100
O	0.46905700	2.53375600	3.17779000	O	-5.74175200	-0.22640000	-0.56960000
O	0.59631500	4.05206000	-0.52728900	H	-5.21278800	-1.05375500	-0.62646400
O	1.75632000	-3.51238600	-1.35855600				

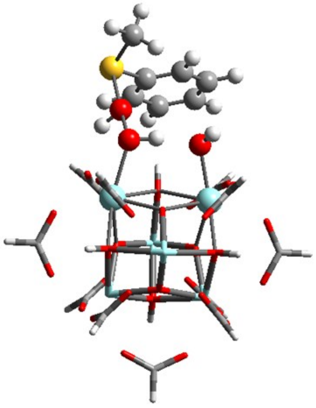

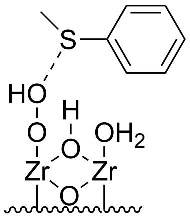

TS for the 1st oxidation ($[Zr_6(\mu_3\text{-}O)_4(\mu_3\text{-}OH)_4(\mu_1\text{-}OOH)(\mu_1\text{-}OH_2)(HCOO)_{11}] + C_6H_5SCH_3$)

C	2.70214900	2.75830700	0.83131200	Zr	0.63668900	0.49652000	2.08421200
C	-0.90218400	3.11037900	3.28624300	Zr	0.73727800	-1.94101900	-0.57113100
C	-0.82545100	-1.43906100	4.30613000	Zr	0.67562300	1.55516400	-1.35511200
C	-0.79868300	4.42122500	-0.92206400	Zr	-2.28848900	1.93944700	0.58388800
C	-4.52020100	1.76434300	-1.77801200	Zr	-2.23249400	-1.54846800	1.36871400
C	-0.68411700	-4.38660500	1.07738200	Zr	-2.17595800	-0.48414400	-2.04355000
C	-0.55358200	-2.97460300	-3.37317600	H	2.65064100	0.02356300	0.16971200
C	-4.59666300	0.46320400	2.35399100	H	-2.02062800	0.67223200	3.11461000
C	2.91780500	-0.46459000	-2.58654500	H	-1.92649400	2.33636400	-2.21764100
C	-4.45093200	-2.47591800	-0.82860300	H	-1.83276400	-3.09805800	-0.98725600
C	-0.63840900	1.27131900	-4.32296400	O	2.33998700	-0.61663000	2.60211700
O	2.47585500	-2.47458900	0.71127800	H	2.26742500	-1.01340800	3.48308200
O	2.35363500	2.64552400	-0.37984100	H	2.51078000	-1.84536200	1.49977300
O	2.23024500	2.14312200	1.81438600	H	-0.91536900	3.90798500	4.05895900
O	0.06522200	-0.59818100	4.01802600	H	-5.56968700	0.56992800	2.87872400
O	0.00668200	2.24561900	3.38509600	H	-5.47326900	2.16366200	-2.18475400
O	-1.66086800	0.48175300	2.23810400	H	-0.57315400	1.53722600	-5.39935200
O	1.68544800	0.05370300	0.08871300	H	-0.46206600	-3.67113400	-4.23306500
O	-0.22966600	1.64539400	0.50910000	H	-5.38745300	-3.03932600	-1.02555800
O	-0.17245400	-1.25101700	1.17689900	H	-0.81758400	-1.83534100	5.34389100
O	-1.80864700	3.16580000	2.41069100	H	3.52192900	3.47997100	1.03477100
O	-1.73205800	-1.87727700	3.54795800	H	-0.63332600	-5.45203500	1.38689700
O	-1.60168700	1.67854900	-1.58848500	H	-0.77676500	5.51600500	-1.10766400
O	-4.11729400	1.50896600	1.84150900	H	3.77954000	-0.58918600	-3.27558600
O	-1.74548300	3.99039300	-0.21202100	O	4.14078600	-2.14510800	0.18144700
O	-4.06853000	2.33173600	-0.74746500	H	3.83963000	-2.09685700	-0.75314100
O	-2.57920600	-0.03980100	-0.04132500	S	6.30320800	-1.82581100	-0.36272200
O	-1.53488200	-2.22229900	-0.70702300	C	6.74090800	-2.58148600	1.22112800
O	2.53763100	-1.50230400	-1.97012200	H	6.64586900	-3.66370400	1.06341100
O	0.21736400	-3.98092300	0.30001200	H	7.77723700	-2.33142700	1.48465800
O	0.31793000	-3.08284800	-2.46874600	H	6.03953000	-2.26494700	2.00341400
O	-0.12286700	-0.35839700	-1.64213100	C	6.52373300	-0.08030400	-0.10972600
O	-4.00217300	-2.52579600	0.34697400	C	6.60272800	0.70506500	-1.27384300
O	-4.08711300	-0.68833800	2.34379900	C	6.60032900	0.52486800	1.15416000
O	-1.64705200	-3.71511300	1.53704300	C	6.75240500	2.08888300	-1.16974600
O	0.22341200	1.78734300	-3.56377200	H	6.55682900	0.23090000	-2.25734600
O	2.43525600	0.68770100	-2.48849700	C	6.75903100	1.91105900	1.24444400
O	0.12058300	3.74323200	-1.45195100	H	6.53900500	-0.06753000	2.06721400
O	-4.00439200	0.79930000	-2.40291000	C	6.83215100	2.69617900	0.08899000
O	-1.52105500	-2.16867700	-3.40314600	H	6.81564000	2.69323600	-2.07771200
O	-3.94847200	-1.86368200	-1.80932300	H	6.82373500	2.37828200	2.23003300
O	-1.57350100	0.49281900	-3.99398700	H	6.95629500	3.77855400	0.16874900

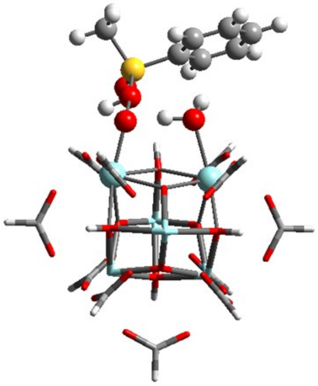

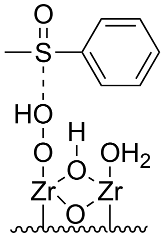

TS for the 2nd oxidation ($[Zr_6(\mu_3\text{-}O)_4(\mu_3\text{-}OH)_4(\mu_1\text{-}OOH)(\mu_1\text{-}OH_2)(HCOO)_{11}] + C_6H_5S(O)CH_3$)

C	-2.87487300	1.65258300	1.93071900
C	0.37205900	4.38684100	1.02597900
C	0.37265800	2.96482700	-3.40792500
C	0.86434500	1.53472300	4.24698200
C	4.74542600	-0.14424300	2.24501300
C	0.71218200	-1.27789400	-4.34458900
C	1.17184900	-4.41076800	-0.86887400
C	4.30161600	2.75316500	-0.96009200
C	-2.38222000	-2.96689800	1.18023100
C	4.65178500	-1.48286300	-1.87100400
C	1.25565800	-3.00315200	3.31975200
O	-2.35777800	-1.21198700	-2.23183700
O	-2.29158900	0.71935700	2.53853800
O	-2.55458400	2.15793900	0.81912600
O	-0.48536600	3.01900600	-2.48778400
O	-0.51494500	3.89260600	0.27946000
O	1.41305800	2.29132300	-0.75677800
O	-1.58517800	-0.23187700	0.12259100
O	0.18167300	1.24196700	1.15556900
O	0.10927100	0.32185500	-1.66614200
O	1.40970800	3.81515800	1.45083500
O	1.38986900	2.22171700	-3.45829800
O	1.81912700	-0.35090600	2.20809700
O	3.87244600	2.79586700	0.22581700
O	1.73915800	2.02235200	3.47940200
O	4.15753600	0.96946600	2.23473100
O	2.62563300	0.19794000	-0.09482100
O	1.73783600	-1.60914400	-1.60057900
O	-2.06378900	-2.97506400	-0.03906000
O	-0.09420100	-1.85737400	-3.57679700
O	0.18435100	-3.82883100	-1.38456100
O	0.42303500	-1.65091300	0.56959400
O	4.05901800	-0.56084400	-2.49140500
O	3.82898600	2.08456900	-1.91515600
O	1.59053000	-0.42710200	-4.02836400
O	0.29557300	-2.19551300	3.42905500
O	-2.00466000	-2.14494900	2.05539900
O	0.03150600	0.63273900	3.97310100
O	4.32909100	-1.22617500	1.75625800
O	2.09935400	-3.88841900	-0.18948000
O	4.26072000	-2.07007700	-0.82757600
O	2.14019400	-3.01741100	2.42207800
Zr	-0.81942600	1.82825500	-0.57860400
Zr	-0.58310700	-1.67319500	-1.33931400
Zr	-0.45432000	-0.53018800	2.07632700
Zr	2.22036300	1.70348900	1.29897900
Zr	2.13978500	0.57739900	-2.09274000
Zr	2.49007000	-1.79978000	0.54790400
H	-2.54541100	-0.37114800	0.05122500
H	1.63443300	3.18249100	-1.05811700
H	2.20408300	-0.50462700	3.08111100
H	2.10026600	-2.24899000	-2.22742200
O	-2.58911600	1.27352600	-1.94529300
H	-3.47725900	1.44187300	-1.59669700
H	-2.54052500	0.23853800	-2.16876600
H	0.22487300	5.44296700	1.33637900
H	5.18949300	3.38148300	-1.18443600
H	5.73583000	-0.17581600	2.74752900
H	1.33769000	-3.78389500	4.10568000
H	1.24534900	-5.50710700	-1.03387600
H	5.62157500	-1.81999300	-2.29495300
H	0.22261900	3.65444500	-4.26574400
H	-3.77590500	2.07744700	2.42113200
H	0.65612800	-1.54312100	-5.42245300
H	0.83391600	1.94267800	5.27961600
H	-3.08857400	-3.75435200	1.51837100
O	-3.92297100	-1.29730800	-1.14293100
H	-3.56129600	-2.19085400	-0.95284500
S	-5.65746800	-1.47342400	0.03734200
C	-6.87070500	-2.44392000	-0.89420900
H	-6.51868700	-3.48364200	-0.86400000
H	-7.83871400	-2.33304400	-0.38716700
H	-6.90125300	-2.06907900	-1.92519500
C	-6.26091500	0.21199800	-0.07234500
C	-6.65416600	0.83064600	1.11713900
C	-6.26783900	0.88394300	-1.30212100
C	-7.08319000	2.16036200	1.06806900
H	-6.62439400	0.27571400	2.05634900
C	-6.70122300	2.21201000	-1.33051800
H	-5.95152600	0.38735600	-2.22187300
C	-7.10539200	2.84811500	-0.14959300
H	-7.39980400	2.65839500	1.98714500
H	-6.72024600	2.75158800	-2.27981000
H	-7.43910500	3.88771900	-0.18059500
O	-5.64861400	-1.92077700	1.46523600

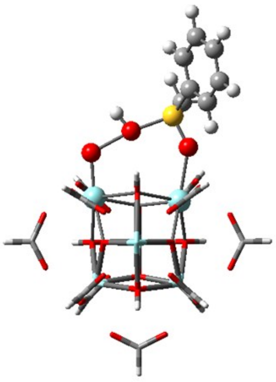

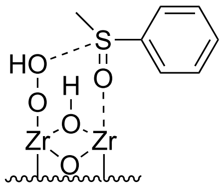

Alternative TS 1 for the 2nd oxidation ($[Zr_6(\mu_3\text{-}O)_4(\mu_3\text{-}OH)_4(\mu_1\text{-}OOH)(\mu_1\text{-}C_6H_5S(O)CH_3)(HCOO)_{11}]$)

C	2.49481900	-3.16498900	-0.02442400
C	0.78473900	-1.92886300	-3.80060000
C	1.57432400	2.55521000	-2.90532100
C	-1.45942600	-4.38114500	-0.94775000
C	-4.93161900	-1.30594500	-1.04228800
C	-0.02103700	4.45183700	0.73033600
C	-2.18764200	1.80051400	3.88940200
C	-2.71679900	1.12861900	-3.88448700
C	0.83899300	-1.27138700	4.06389700
C	-4.19998700	2.83881800	-0.18387900
C	-2.99863500	-2.51020300	3.03059600
O	2.17005700	1.88176800	2.54401400
O	1.57023200	-3.31761600	0.81971400
O	2.66722100	-2.18580000	-0.78748900
O	2.13684500	1.49455600	-2.52042400
O	1.63391400	-1.29914200	-3.11355300
O	-0.31416700	0.37387100	-2.37617400
O	1.46510600	-0.54693400	1.09694300
O	-0.06657200	-1.51928400	-0.75768700
O	0.52851700	1.37290600	-0.19430000
O	-0.44941800	-2.03132500	-3.57381300
O	0.41669100	2.95210800	-2.61688100
O	-2.35893500	-1.86491500	0.23292600
O	-2.63342400	-0.10673000	-3.64648300
O	-1.85710200	-3.55028800	-1.81155300
O	-4.03030800	-1.63071500	-1.86657300
O	-2.27287500	0.40600000	-0.81937200
O	-1.64765100	2.01013100	0.99708600
O	0.74856500	-0.04561600	3.87635000
O	0.32669100	3.70194000	1.66291900
O	-0.97514800	2.01492000	3.63755600
O	-1.03359100	-0.35031700	1.74099600
O	-3.20684500	3.12567900	-0.90024100
O	-2.24695100	2.06849500	-3.19300800
O	-0.56520700	4.11018300	-0.36545100
O	-1.89684000	-2.98526200	2.64750300
O	0.64590900	-2.19307600	3.21116800
O	-0.94123400	-4.12752600	0.16830700
O	-4.77942400	-0.72970300	0.06248100
O	-3.02315800	1.18980500	3.16862200
O	-4.30109700	1.88428100	0.63376500
O	-3.55865000	-1.45770100	2.62094600
Zr	1.48749800	-0.21578900	-1.14025300
Zr	0.41160500	1.33187200	1.97808300
Zr	-0.31515100	-2.19018100	1.22177200
Zr	-1.81081900	-1.30287500	-1.91155900
Zr	-1.16310200	2.14344100	-1.19735000
Zr	-2.94616300	0.15150200	1.15495600
H	2.29316900	-0.77183400	1.54437300
H	-0.14139000	0.54425200	-3.31166300
H	-2.99926700	-2.58159700	0.33196200
H	-2.01832600	2.81158800	1.38814900
O	3.77102300	0.17147200	-0.89851500
H	1.16673500	-2.44143600	-4.70874100
H	-3.25683200	1.41610600	-4.81176700
H	-5.97229400	-1.56954400	-1.32949600
H	-3.54092000	-3.08613100	3.81054600
H	-2.57253100	2.20114000	4.85229700
H	-5.08535500	3.50451100	-0.27457600
H	2.16821600	3.21053700	-3.57866100
H	3.24099100	-3.98681100	-0.08731300
H	0.15189400	5.54379400	0.85627300
H	-1.59081800	-5.45424400	-1.20426400
H	1.12744800	-1.61659100	5.08194100
S	4.75031200	1.04574100	-0.16269800
C	6.25996400	0.10611800	-0.00789000
C	7.42748300	0.73076000	0.45470500
C	6.19333400	-1.26993400	-0.26409600
C	8.57195400	-0.04941400	0.62098700
H	7.46017000	1.79791300	0.68085000
C	7.35243600	-2.02873300	-0.08736500
H	5.26034000	-1.72369100	-0.60296400
C	8.53522200	-1.42297000	0.35069400
H	9.49492100	0.41975800	0.96749900
H	7.32779500	-3.10047500	-0.29526700
H	9.43572700	-2.02575900	0.48712900
C	5.12142200	2.50103600	-1.15192000
H	5.84915600	3.11583800	-0.60650700
H	5.50935500	2.16300500	-2.12217700
H	4.16507400	3.02759700	-1.25604200
O	3.58552900	1.48774900	1.27124200
H	4.06814200	2.04416500	1.91385200

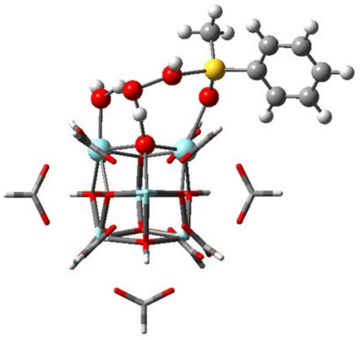

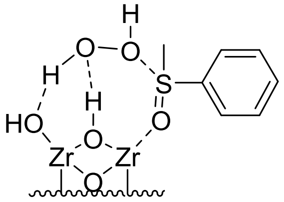

Alternative TS 2 for the 2nd oxidation $([Zr_6(\mu_3\text{-}O)_4(\mu_3\text{-}OH)_4(\mu_1\text{-}OH)(\mu_1\text{-}C_6H_5S(O)CH_3)(HCOO)_{11}]) + H_2O_2$

C	-3.05535700	0.30082000	-2.37926900
C	-2.14632200	-3.44787600	-0.22563700
C	-1.38372600	-1.11725500	3.79332100
C	0.02680300	-2.28802500	-3.81792900
C	4.04721100	-2.80763300	-1.49485700
C	1.36632400	2.16839700	3.91894000
C	3.72338700	3.39701000	0.07272200
C	1.86136400	-3.90891600	2.07782100
C	0.08721100	3.82941000	-2.24776100
C	4.70147100	-0.61220900	2.20909800
C	3.07433800	1.21029100	-3.68776800
O	-0.92538800	3.64056800	1.31352700
O	-2.00238900	0.63481200	-2.98243500
O	-3.15442200	-0.11238400	-1.19961400
O	-2.07424000	-0.87811800	2.77726300
O	-2.57412400	-2.36045400	0.24006500
O	-0.13882000	-1.90355000	1.25249800
O	-0.99058500	1.49729600	-0.54489100
O	-0.44188000	-0.94025300	-1.03002500
O	-0.01330300	0.59052800	1.58195400
O	-0.96536300	-3.72187200	-0.57694100
O	-0.12214600	-1.17172600	3.87089800
O	1.86999900	-0.89122000	-2.02212900
O	1.52194000	-4.00179500	0.86736800
O	0.40371000	-2.98661600	-2.83684600
O	2.90029400	-3.31969900	-1.37688900
O	2.11571000	-1.19246500	0.44543800
O	2.45337000	1.10720100	1.38506500
O	0.40335200	3.92853400	-1.04250900
O	1.05712300	2.86876600	2.92319500
O	2.57471300	3.63550700	0.52123400
O	1.53421800	1.35081700	-0.95122300
O	3.65165200	-0.80548900	2.87723500
O	1.88031300	-2.86872800	2.78436600
O	1.60035300	0.92779800	3.94282100
O	1.82499500	1.14213500	-3.79257900
O	-0.13768300	2.76483000	-2.89041300
O	-0.09213400	-1.03838400	-3.86361100
O	4.37008300	-1.60768800	-1.30050700
O	4.17684600	2.28945000	-0.33285800
O	4.78163900	-0.21776000	1.01680000
O	3.77906300	0.90691000	-2.68383500
Zr	0.64858500	2.38515800	0.68142000
Zr	0.13449700	0.63211200	-2.30076300
Zr	-1.61598000	-0.28427300	0.53684500
Zr	0.91978700	-2.47880200	-0.68879500
Zr	1.44720800	-0.67734700	2.36556300
Zr	3.23926200	0.24651900	-0.59047200
H	-1.90476000	2.63684600	-0.78916600
H	-0.54800400	-2.62112600	1.75380400
H	2.27487400	-1.20902300	-2.83961700
H	3.10075900	1.57590000	1.92777100
O	-3.80993100	0.25544300	1.34911600
H	-2.88943300	-4.26770600	-0.33145500
H	2.17107300	-4.85262400	2.57603800
H	4.86095500	-3.49490800	-1.81167000
H	3.63008200	1.57001800	-4.58104700
H	4.43087500	4.25401300	0.03616800
H	5.66259900	-0.80429000	2.73285800
H	-1.93327400	-1.31661100	4.73983700
H	-4.00030500	0.38074300	-2.96071300
H	1.45083800	2.69770100	4.89333400
H	-0.21855500	-2.84517400	-4.74834800
H	-0.01207500	4.77535700	-2.82439600
S	-4.98487300	1.04406800	0.80434800
C	-6.20966400	-0.10950700	0.17329300
C	-7.43772300	0.38653300	-0.28491000
C	-5.87650100	-1.46667700	0.11200800
C	-8.37615700	-0.52073700	-0.77970800
H	-7.67012600	1.45343500	-0.26190800
C	-6.83251100	-2.35508900	-0.38829700
H	-4.89392400	-1.81441000	0.43453900
C	-8.07528700	-1.88736300	-0.82880000
H	-9.34296200	-0.15589300	-1.13266500
H	-6.59889000	-3.42107300	-0.43553100
H	-8.81316900	-2.59120500	-1.22046300
C	-5.76993000	1.81379100	2.23037000
H	-6.65317200	2.36901100	1.88793800
H	-6.03664200	1.02340400	2.94429300
H	-5.01832300	2.49889300	2.64320700
H	-0.99376500	3.80812000	2.26325900
H	-2.04075000	3.76110500	0.23711700
O	-2.46875000	3.52086700	-0.66661400
O	-3.87061700	2.51665200	-0.07620100
H	-4.48067600	2.96063000	-0.70025400

S10. Author contribution

R.L. and S.T.N. formulated the initial project, and conceived experiments presented herein. R.L. conducted all the experiments. H.C. carried out the calculations for the catalyzed reactions. M.L.M. carried out the calculations for uncatalyzed reaction. M.L. synthesized the **BzOH-UiO-66** for recyclability and carried out the SEM imaging of **BzOH-UiO-66,** and **HCOOH-UiO-66**. R.Q.S. and S.T.N. supervised the project. R.L. and H.C. wrote the initial drafts of the paper. R.L. and S.T.N. finalized the manuscript with inputs from all co-authors.

S11. References

S1. Troya, D. *J. Phys. Chem. C.* **2016**, *120*, 29312-29323.
S2. Becke, A. D. *J. Chem. Phys.* **1993**, *98*, 5648-5652.
S3. Lee, C.; Yang, W.; Parr, R. G. *Phys. Rev. B* **1988**, *37*, 785-789.
S4. Weigend, F.; Ahlrichs, R. *Phys. Chem. Chem. Phys.* **2005**, *7*, 3297-3305.
S5. Hay, P. J.; Wadt, W. R. *J. Chem. Phys.* **1985**, *82*, 270-283.
S6. Cossi, M.; Barone, V.; Cammi, R.; Tomasi, J. *Chem. Phys. Lett.* **1996**, *255*, 327-335.
S7. Grimme, S.; Antony, J.; Ehrlich, S.; Krieg, H. *J. Chem. Phys.* **2010**, *132*, 154104.
S8. Becke, A. D.; Johnson, E. R. *J. Chem. Phys.* **2005**, *123*, 154101.
S9. Schaate, A.; Roy, P.; Godt, A.; Lippke, J.; Waltz, F.; Wiebcke, M.; Behrens, P. *Chem. Eur. J* **2011**, *17*, 6643-6651.
S10. Nguyen, H. G. T.; Schweitzer, N. M.; Chang, C.-Y.; Drake, T. L.; So, M. C.; Stair, P. C.; Farha, O. K.; Hupp, J. T.; Nguyen, S. T. *ACS Catal.* **2014**, *4*, 2496-2500.
S11. Thornburg, N. E.; Liu, Y.; Li, P.; Hupp, J. T.; Farha, O. K.; Notestein, J. M. *Catal. Sci. Technol.* **2016**, *6*, 6480-6484.
S12. Kickelbick, G.; Wiede, P.; Schubert, U. *Inorg. Chim. Acta* **1999**, *284*, 1-7.
S13. Harman, D. G.; Ramachandran, A.; Gracanin, M.; Blanksby, S. J. *J. Org. Chem.* **2006**, *71*, 7996-8005.
S14. Shearer, G. C.; Chavan, S.; Bordiga, S.; Svelle, S.; Olsbye, U.; Lillerud, K. P. *Chem. Mater.* **2016**, *28*, 3749-3761.
S15. Atzori, C.; Shearer, G. C.; Maschio, L.; Civalleri, B.; Bonino, F.; Lamberti, C.; Svelle, S.; Lillerud, K. P.; Bordiga, S. *J. Phys. Chem. C.* **2017**, *121*, 9312-9324.
S16. Katz, M. J.; Brown, Z. J.; Colon, Y. J.; Siu, P. W.; Scheidt, K. A.; Snurr, R. Q.; Hupp, J. T.; Farha, O. K. *Chem. Commun.* **2013**, *49*, 9449-9451.
S17. Faccioli, F.; Bauer, M.; Pedron, D.; Sorarù, A.; Carraro, M.; Gross, S. *Eur. J. Inorg. Chem.* **2015**, *2015*, 210-225.